Published in final edited form as:

Cell Rep. 2022 August 23; 40(8): 111259. doi:10.1016/j.celrep.2022.111259.

Hepatocyte Rap1a contributes to obesity- and statin-associated hyperglycemia

Yating Wang[1,2], **Stefano Spolitu**[1], **John A. Zadroga**[1], **Amesh K. Sarecha**[1], **Lale Ozcan**[1,3,*]

[1]Department of Medicine, Columbia University Irving Medical Center, New York, NY 10032, USA

[2]Department of Cardiology, The Second Xiangya Hospital, Central South University, Changsha, China

[3]Lead contact

SUMMARY

Excessive hepatic glucose production contributes to the development of hyperglycemia and is a key feature of type 2 diabetes. Here, we report that activation of hepatocyte Rap1a suppresses gluconeogenic gene expression and glucose production, whereas Rap1a silencing stimulates them. Rap1a activation is suppressed in obese mouse liver, and restoring its activity improves glucose intolerance. As Rap1a′s membrane localization and activation depends on its geranylgeranylation, which is inhibited by statins, we show that statin-treated hepatocytes and the human liver have lower active-Rap1a levels. Similar to Rap1a inhibition, statins stimulate hepatic gluconeogenesis and increase fasting blood glucose in obese mice. Geranylgeraniol treatment, which acts as the precursor for geranylgeranyl isoprenoids, restores Rap1a activity and improves statin-mediated glucose intolerance. Mechanistically, Rap1a activation induces actin polymerization, which suppresses gluconeogenesis by Akt-mediated FoxO1 inhibition. Thus, Rap1a regulates hepatic glucose homeostasis, and blocking its activity, via lowering geranylgeranyl isoprenoids, contributes to statin-induced glucose intolerance.

In brief

Wang et al. show that activation of hepatic Rap1a suppresses gluconeogenic gene expression and improves glucose intolerance via Akt-mediated FoxO1 inhibition. Statins lower intracellular isoprenoid levels and inhibit Rap1a activation, which contributes to their hyperglycemic effect.

*Correspondence: lo2192@cumc.columbia.edu.

AUTHOR CONTRIBUTIONS

Y.W., S.S., J.A.Z., and A.S. designed and performed the experiments, analyzed the data, interpreted results, and edited the manuscript. L.O. conceived and supervised the project, designed experiments, analyzed data, interpreted results, and wrote the manuscript.

SUPPLEMENTAL INFORMATION

Supplemental information can be found online at https://doi.org/10.1016/j.celrep.2022.111259.

DECLARATION OF INTERESTS

The authors declare no competing interests.

INCLUSION AND DIVERSITY

One or more of the authors of this paper self-identifies as an underrepresented ethnic minority in science. One or more of the authors of this paper self-identifies as a member of the LGBTQ+ community.

These findings identify a role of hepatic Rap1a in obesity- and statin-associated glucose homeostasis.

Graphical Abstract

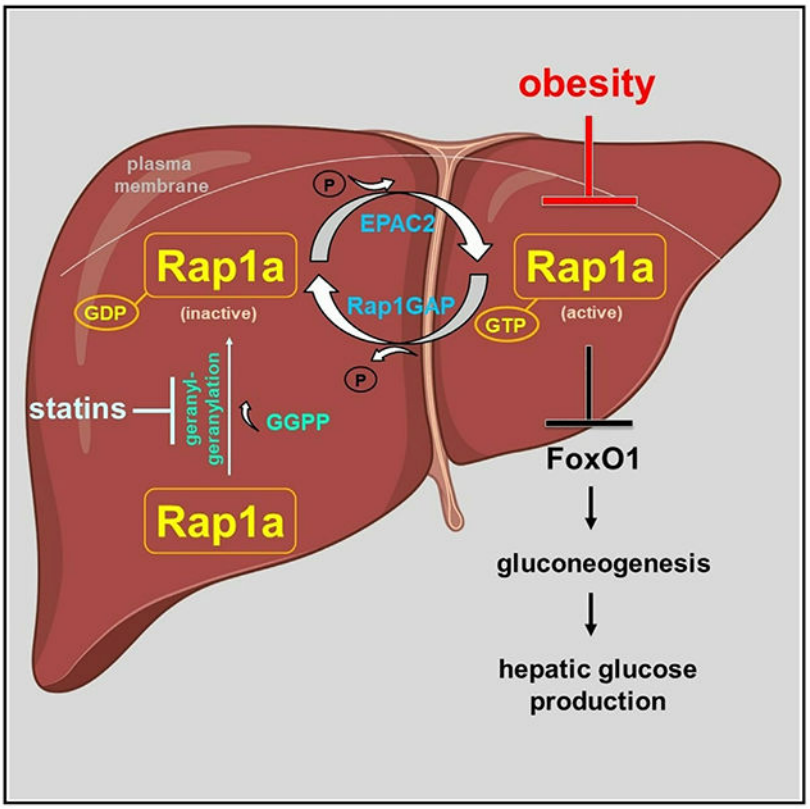

INTRODUCTION

A major cause of hyperglycemia in type 2 diabetes (T2D) is enhanced hepatic glucose production (HGP), which results from an increase in gluconeogenesis (Lin and Accili, 2011; Magnusson et al., 1992). Several factors, including the availability of substrates and an imbalance between glucagon and insulin action, contribute to this process (Petersen et al., 2017). Glucagon plays a major role in hepatic gluconeogenesis, in part by increasing cyclic AMP (cAMP) and intracellular calcium levels, which results in increased expression of two key gluconeogenic enzymes, phosphoenol pyruvate carboxykinase (PCK1) and glucose 6 phosphatase (G6PC) (Ramnanan et al., 2011). A number of transcription factors and coactivators including forkhead box O1 (FoxO1) and cAMP response element-binding protein (CREB) activate and stimulate the transcription of these gluconeogenic genes in T2D; however, little is known about the endogenous regulatory mechanisms that prevent aberrant activation of this pathway.

One of the major complications of T2D is to increase the risk for developing cardiovascular disease, and the majority of T2D patients use cholesterol-lowering statin drugs (Benjamin et al., 2018). By inhibiting HMG-CoA reductase, the rate-limiting enzyme of the mevalonate

pathway, statins decrease hepatic cholesterol synthesis and increase low-density lipoprotein (LDL) receptor (LDLR) levels, which results in enhanced LDL clearance from the plasma (Baigent et al., 2005; Goldstein and Brown, 2015). Although they are generally considered to be safe and well-tolerated, recent evidence from meta-analyses of major statin trials showed that statin therapy is associated with a ~10%–11% increased risk for new-onset T2D (Casula et al., 2017; Ridker et al., 2008; Sattar et al., 2010). The risk is dose-dependent and increased by close to 46% in older patients and patients with pre-existing risk factors for T2D (Cederberg et al., 2015; Crandall et al., 2017; Preiss et al., 2011). These results prompted US Food and Drug Administration (FDA) to approve labeling changes in statins to include a warning about the possibility of increased blood sugar (FDA, 2012). Interestingly, loss-of-function mutations in *HMGCR*, which encodes HMG-CoA reductase, are also associated with increased incidence of new-onset T2D, suggesting that the diabetogenic effect of statins is “on-target” (Ference et al., 2016; Swerdlow et al., 2015). Despite these findings, the cellular and molecular mechanisms that link statins to increased T2D risk are largely unknown. Besides lowering plasma LDL levels, statins have additional actions, which involve inhibition of the mevalonate pathway. Mevalonate is the precursor for the generation of farnesyl pyrophosphate and geranylgeranyl pyrophosphate (GGPP) isoprenoids that are required for the prenylation and activation of a subset of proteins, including the small GTPase, Ras-related protein 1A (Rap1a).

Rap1a belongs to the Ras superfamily of GTPases and cycles between an inactive GDP-bound form and an active GTP-bound form (Gloerich and Bos, 2011; Kitayama et al., 1989; Wittchen et al., 2011). Post-translational covalent attachment of geranylgeranyl isoprenoid chain to Rap1a results in its membrane localization, where exchange protein directly activated by cAMP 2 (Epac2) activates Rap1a via GTP loading (Bos et al., 2007). GTPase-activating proteins, such as Rap1GAP, stimulate GTP hydrolysis and thereby inactivate Rap1a. We previously reported a role for Rap1a in metabolic disease and showed that activation of Rap1a lowers plasma LDL via decreasing proprotein convertase subtilisin-kexin type 9 (PCSK9) (Spolitu et al., 2019). However, much less is known about the contribution of hepatic Epac2 or Rap1a to glucose homeostasis.

In the present study, we explored the role of Rap1a in liver glucose metabolism and show that hepatic Rap1a suppresses gluconeogenesis and glucose production via regulating actin polymerization and Akt-mediated FoxO1 inhibition. Hepatic Rap1a activity is significantly lower in obese mice, and overexpression of a constitutively active mutant form of Rap1a in the liver lowers blood glucose and improves glucose intolerance. Given that geranylgeranylation is required for Rap1a to become fully activated, we found that Rap1a activity is also decreased in statin-treated primary hepatocytes and human liver samples from statin users. Accordingly, statin treatment stimulates glucose production *in vitro* and further increases fasting blood glucose and worsens glucose intolerance in obese mice. Adding back geranylgeranyl isoprenoids restores hepatic Rap1a activity and improves hyperglycemia. These findings identify Rap1a as an important mediator of obesity- and statin-induced glucose intolerance.

RESULTS

Inhibition of Epac2 or Rap1a stimulates gluconeogenesis and increases HGP

A recent GWAS study demonstrated that variants in *RAPGEF4*, which encodes EPAC2, are associated with fasting blood glucose in East Asians; however, the functional significance of this finding is not known (Hwang et al., 2015). To test whether Epac2 and its downstream effector, Rap1a, contribute to hepatic glucose metabolism, we tested their effects on the expression of gluconeogenic genes, *G6pc* and *Pck1*. Upon stimulation of freshly isolated primary mouse hepatocytes with forskolin, a glucagon mimetic and potent adenylate cyclase activator, and dexamethasone, which downregulates cAMP-phosphodiesterase (Manganiello and Vaughan, 1972), we observed that the expression of *G6pc* and *Pck1* was further increased in hepatocytes treated with siRNAs against Epac2 or Rap1a (Figures 1A, 1C, and 1D). Accordingly, glucagon treatment resulted in an increase in *G6pc* and *Pck1* mRNA levels in Rap1a-deficient hepatocytes versus control (Figure 1F). Similar data were obtained in a mouse hepatocyte cell line, AML-12 cells (Figures S1A and S1B). Consistent with an increase in the expression of gluconeogenic genes, we observed a further increase in glucose release in cells lacking Epac2 or Rap1a after forskolin and dexamethasone stimulation (Figures 1B and 1E). To assess the functional role of Rap1a in hepatic glucose metabolism *in vivo*, we deleted liver Rap1a by injecting diet-induced obese (DIO) $Rap1a^{fl/fl}$ mice with adeno-associated virus-8 encoding Cre recombinase driven by the hepatocyte-specific thyroxine-binding globulin promoter (AAV8-TBG-Cre), and AAV8-TBG-Gfp-treated $Rap1a^{fl/fl}$ mice served as controls. The TBG-Cre treatment successfully silenced Rap1a in the liver (Figure 1G) without altering body weight (Figure 1H). In line with the *in vitro* data, DIO mice that lack hepatocyte Rap1a had higher fasting blood glucose levels (Figure 1I) and hepatic *Pck1* expression (Figure 1J) without a change in plasma insulin levels (Figure 1K). Consistent with these results, hepatocyte Rap1a-deficient mice also showed greater blood glucose excursions than control mice upon glucose challenge (Figure 1L). We next evaluated the effect of activated hepatic Rap1a by treating primary hepatocytes with a plasmid encoding a constitutively active Rap1a mutant (CA-Rap1a). CA-Rap1a possesses an amino acid substitution, Q63E, which results in constitutive GTP-binding, so the mutated form of Rap1a is always active and unable to be downregulated by Rap1GAP (Spolitu et al., 2019; Wittchen et al., 2011). Compared with control plasmid-treated cells, CA-Rap1a-overexpressing cells had lower *G6pc* and *Pck1* mRNA expression and showed 50% decrease in glucose production upon forskolin and dexamethasone treatment (Figures S1C and S1D). These results suggested that activation of Rap1a suppresses gluconeogenesis.

To further evaluate the physiologic relevance of Rap1a-mediated gluconeogenesis suppression, we checked hepatic Rap1a activity during the transition from a fed to fasting state in WT mice. Consistent with an increase in hepatic gluconeogenic gene expression, we found that the GTP-bound, active-Rap1a levels in the liver were lower after 6 h of fasting (Figure S2A), which still remained low after 14 and 24 h of fasting (Figures S2B and S2C). Fasting, however, did not increase the levels of hepatic phosphorylated CREB as reported before (Stern et al., 2019). These data support the hypothesis that Rap1a negatively

regulates gluconeogenesis, and the major function of Rap1a in hepatic glucose metabolism is to inhibit the aberrant activation of HGP.

Activation of Rap1a is suppressed in obese mice liver, and restoring Rap1a activity lowers blood glucose and improves glucose intolerance in obese mice

Because Rap1a activation lowers gluconeogenesis and glucose production (Figures S1C and S1D), we next asked if Rap1a is inhibited in mouse models of T2D and insulin resistance where gluconeogenesis and HGP are elevated. In genetically obese and diabetic *db/db* mice liver, we found that the GTP-bound, active Rap1a levels were significantly decreased compared with heterozygous *db*/+ controls (Figure 2A). Similar data were obtained in the livers of DIO mice versus their low-fat-fed controls (Figure 2B). We then restored hepatic Rap1a activity by treating *db/db* mice with AAV8-TBG-CA-Rap1a, which specifically expresses the constitutively active Rap1a in hepatocytes. Despite similar body weight (Figure 2C), we observed that overexpressing TBG-CA-Rap1a in *db/db* mice liver lowered fasting blood glucose (Figure 2D), improved glucose intolerance (Figure 2E), and lowered hepatic gluconeogenic gene expression (Figure 2F), without affecting plasma insulin levels (Figure 2G). Similar results were obtained when DIO mice were treated with adeno-CA-Rap1a (Figures 2H–2L). These combined data provide evidence that Rap1a regulates gluconeogenesis and HGP and contributes to glucose homeostasis *in vivo*.

Statins inhibit Rap1a in isolated hepatocytes and the human liver

Attachment of GGPP to Rap1a results in its membrane localization and Epac2-mediated GTP loading, which supports the importance of the mevalonate pathway in Rap1a′s activation (Goody et al., 2017; Jaskiewicz et al., 2018). Interestingly, a previous report showed that statin treatment of skeletal muscle cells *in vitro* lowers Rap1a isoprenylation, which was suggested as a plausible mechanism to explain statin-mediated myotoxicity (Jaśkiewicz et al., 2018). Because the liver is the primary organ responsible for the metabolism and action of statins, we hypothesized that one mechanism by which statins increase the risk for new-onset T2D is their ability to lower GGPP, inhibit Rap1a, and aberrantly activate HGP. As a first step in investigating this hypothesis, we determined whether statin treatment of hepatocytes inhibits Rap1a′s prenylation and membrane localization. We found that treatment of primary mouse hepatocytes with two potent statins in clinical use, simvastatin or rosuvastatin, significantly lowered membrane Rap1a protein, without decreasing the total cellular Rap1a levels (Figures 3A and 3B). Further, the decrease in membrane localization of Rap1a was associated with inhibition of its activity, as rosuvastatin treatment lowered GTP-bound, active Rap1a levels (Figure 3C). To study the relevance to humans, we obtained human liver specimens from the Liver Tissue Cell Distribution System sponsored by the National Institutes of Health. Strikingly, we observed that the GTP-bound, active Rap1a levels were significantly decreased in the livers of human patients on statin therapy compared with their disease-, age-, and sex-matched controls who are not using statins (Figure 3D). We obtained similar results from liver samples of another set of patients that are matched for age, sex, and body mass index (Figure 3E). Thus, statin treatment inhibits Rap1a activity in mouse hepatocytes and the human liver.

Statins increase gluconeogenesis in WT but not in Rap1a-deficient hepatocytes

Given that statins lower Rap1a activity and Rap1a inhibition increases HGP, we then sought to investigate whether an increase in hepatic gluconeogenesis is involved in the diabetogenic effects of statins. We observed that treatment of primary mouse hepatocytes with different statins, including, simvastatin, rosuvastatin, or fluvastatin, increased *G6pc* and *Pck1* mRNAs (Figures 4A, S3A, S3C, and S3D). Consistent with an increase in gluconeogenic gene expression, glucose production was also increased upon statin treatment (Figures 4B and S3B). Moreover, rosuvastatin treatment of metabolism-qualified primary human hepatocytes resulted in an increase in gluconeogenic gene expression, which provides information about the human relevance of our murine hepatocyte studies (Figures 4C and 4D). To understand whether inhibition of Rap1a is one of the major mechanisms by which statins induce gluconeogenic gene expression, we incubated control or si-Rap1a-treated hepatocytes with rosuvastatin. Confirming our above results, both silencing Rap1a or rosuvastatin treatment alone increased *G6pc* mRNA (Figure 4E). Importantly, rosuvastatin's ability to increase *G6pc* and *Pck1* mRNAs was abolished in Rap1a-silenced hepatocytes (Figures 4E and 4F). These results support the idea that inhibition of Rap1a acts in the same pathway as statins and is a major mechanism by which statins increase gluconeogenesis. To show the relevance of statin treatment on glucose metabolism regulation *in vivo*, we treated DIO mice with a high-fat diet containing 0.02% simvastatin (w/w) for 12 weeks and observed that both groups gained similar weight during the treatment (Figure 4G). As expected, statin treatment resulted in an increase in the mRNA expression of Srebp2 target genes, including *Hmgcs* and *Hmgcr* in the liver (Figure S3E). Similar to hepatic Rap1a silencing, we found that statin-treated obese mice had higher fasting blood glucose, increased gluconeogenic gene expression in the liver, and they were more glucose intolerant compared with control mice, without alterations in plasma insulin levels (Figures 4H–4L).

Statins lower plasma LDL via increasing LDLR protein levels and paradoxically increase the expression of PCSK9 (Goldstein and Brown, 2009; Sahebkar et al., 2015; Taylor and Thompson, 2016). To understand the involvement of LDLR and PCSK9 in statin-mediated regulation of hepatocyte glucose metabolism, we treated primary hepatocytes isolated from $Ldlr^{-/-}$ and $Pcsk9^{-/-}$ mice with rosuvastatin. Similar to WT cells, we observed an increase in *G6pc* mRNA levels and glucose production in LDLR- and PCSK9-deficient hepatocytes treated with rosuvastatin compared with vehicle (Figures S3F–S3I). Thus, statins stimulate gluconeogenesis and increase glucose production, and this regulation is independent of LDLR and PCSK9.

GGPP supplementation restores Rap1a activity and improves statin-induced glucose intolerance in obese mice

Inhibition of HMG-CoA reductase by statins suppresses GGPP isoprenoid synthesis, which is required for Rap1a to become activated (Jaskiewicz et al., 2018). Because statin treatment or Rap1a inhibition increases gluconeogenesis, we reasoned that a decrease in intracellular GGPP levels is involved in statin-mediated gluconeogenic gene induction. To test this, we put back intracellular GGPP in statin-treated hepatocytes by incubating them with exogenous GGPP. We found that this treatment brought back plasma membrane-localized Rap1a to vehicle-treated levels, suggesting that Rap1a prenylation was restored (Figure

5A). Consistent with the restoration of Rap1a′s membrane localization, GGPP treatment abrogated the increase in *G6pc* and *Pck1* mRNA levels conferred by statin treatment in isolated hepatocytes (Figure 5B). Of note, GGPP treatment did not inhibit simvastatin-induced *Hmgcr* and *Hmgcs* mRNAs (Figure S4A), suggesting that induction of Srebp2 by statins was intact and unaffected by GGPP restoration. We next sought to determine if GGPP supplementation in statin-treated obese mice could lower HGP and improve glucose intolerance. Accordingly, we fed DIO mice with a high-fat diet containing 0.02% simvastatin (w/w) for 12 weeks. Mice were then administered with GGPP precursor, geranylgeraniol (GGOH, 100 mg/kg), or vehicle control by daily gavage while still receiving the statin-containing diet (Gibbs et al., 1999). After 3 weeks of treatment, we observed higher hepatic active-Rap1a levels (Figure S4B), lower fasting blood glucose (Figure 5C), improved glucose intolerance (Figure 5D), and decreased hepatic gluconeogenic gene expression (Figure 5E), without a change in body weight or plasma insulin levels (Figures 5F and 5G) in the GGOH-supplemented group compared with statin treatment alone. Of note, we did not observe changes in blood glucose, hepatic gluconeogenic gene expression, body weight, or plasma insulin levels in DIO mice treated with GGOH alone (Figures S4C–S4G).

Given that one of the major effects of statins is to decrease cholesterol biosynthesis, we next asked whether lowering of intracellular cholesterol participates in the gluconeogenic effects of statins. For this purpose, we restored intracellular cholesterol levels in statin-treated hepatocytes by incubating them with cholesterol-enriched phospholipid liposomes (Lipo-Chol) (Wang et al., 2020). As expected, increased expression of cholesterol synthesis genes, including *Hmgcr* and *Hmgcs*, upon statin treatment was lowered back to control levels in cells treated with Lipo-Chol and statin together (Figures S5A and S5B). However, restoration of intracellular cholesterol was not able to reverse statin-induced *G6pc* and *Pck1* mRNAs (Figures S5C and S5D). Notably, Lipo-Chol treatment did not affect membrane localization of Rap1a (Figure S5E). These results support the hypothesis that statins inhibit Rap1a activity and increase HGP via lowering GGPP levels, which is independent of a change in intracellular cholesterol content.

Geranylgeranyl transferase-1 inhibition mimics statins and increases hepatocyte gluconeogenesis

Our results thus far suggest that statins inhibit activation of Rap1a and increase HGP, and restoring GGPP levels brings back Rap1a activity and lowers glucose production. Geranylgeranyl transferase 1 (GGT1) covalently attaches GGPP to Rap1a to form a stable thioether bond (Jaskiewicz et al., 2018). This post-translational modification increases Rap1a′s hydrophobicity, which results in Rap1a′s plasma membrane localization (Ghomashchi et al., 1995). To understand the contribution of GGT1 to hepatic glucose metabolism, we used a specific GGT1 inhibitor or silenced *Pggt1b*, the gene encoding GGT1, in primary hepatocytes. Similar to statin treatment or Rap1a silencing, inhibition or silencing of GGT1 increased gluconeogenic gene expression and glucose production in both primary mouse and human hepatocytes (Figures 5H and S6A–S6D). Consistent with a role for GGT1 in gluconeogenesis *in vivo*, treatment of DIO mice with hepatocyte-specific AAV8 encoding short hairpin RNA (shRNA) construct targeting *Pggt1b* resulted in lowering

of hepatic *Pggt1b* mRNA expression by ~50% and increased fasting blood glucose levels in obese mice, without altering body weight or plasma insulin (Figures 5I–5L). It is noteworthy to mention that farnesyl transferase inhibitor, FTI-277, did not affect *G6pc* or *Pck1* mRNA levels in primary mouse hepatocytes (Figure S6E). Collectively, these data suggest that inhibition of GGPP synthesis and Rap1a activity by statins increases gluconeogenesis, which is mimicked by GGT1 inhibition.

Rap1a inhibition or statin treatment increases gluconeogenesis via regulating FoxO1 activity

In an attempt to understand the molecular mechanism(s) by which Rap1a regulates HGP, we first determined whether Rap1a deficiency in primary hepatocytes affects intracellular cAMP levels. We found that both basal and forskolin- and dexamethasone-treated intracellular cAMP levels were similar in Rap1a-deficient or CA-Rap1a-overexpressing cells compared with controls (Figures S7A and S7B). Protein kinase A (PKA) is well known for its ability to stimulate gluconeogenesis via increasing the nuclear localization and activity of CREB and CRTC2 transcription factors (Chrivia et al., 1993; Wang et al., 2012b). We next considered the possibility that Rap1a deficiency may stimulate gluconeogenesis via activating PKA. However, we observed that the levels of both p-CREB and p-PKA substrates, as measures of CREB and PKA activities, respectively, were not increased in Rap1a-silenced hepatocytes versus control (Figure S7C). In support of this finding, mRNA levels of one of the downstream effectors for both CTRC2 and CREB pathways, peroxisome proliferator-activated receptor-γ coactivator-1α (*Pgc1a*) (Herzig et al., 2001), were similar in WT and Rap1a-deficient hepatocytes (Figure S7D). Interestingly, *Pgc1a* mRNA levels were decreased, not increased, in cells treated with simvastatin or rosuvastatin compared with controls (Figure S7E). These results support the idea that Rap1a regulates gluconeogenesis without affecting PKA activity.

Forkhead box O1 (FoxO1) is a major gluconeogenic transcription factor that induces the transcription of *G6pc* and *Pck1* (Pajvani and Accili, 2015). To investigate whether statins or Rap1a inhibition enhance gluconeogenesis via regulating FoxO1, we first measured the mRNA levels of another well-known FoxO1 target gene, *Igfbp1* (Matsumoto et al., 2006). We observed that Rap1a deficiency, statin treatment, or GGT1i treatment increased hepatic *Igfbp1* mRNA levels (Figures 6A, 6B, S7F, and S7G). Glucokinase (encoded by *Gck*) is critical for hepatic glucose utilization and is negatively regulated by FoxOs (Haeusler et al., 2014; Langlet et al., 2017). In support of the role of Rap1a in regulating FoxO1, we found lower *Gck* mRNA levels in Rap1a-deficient DIO liver compared with control (Figure 6C). Likewise, *Gck* mRNA was significantly lower in $Rap1a^{-/-}$ hepatocytes in response to a combination of forskolin, dexamethasone, and insulin treatment, which has been shown to induce *Gck* (Langlet et al., 2017) (Figure S7H). Conversely, CA-Rap1a overexpression increased forskolin + dexamethasone + insulin-induced *Gck* mRNA in WT hepatocytes (Figure S7I). We then addressed whether Rap1a affects FoxO1 ’s transcriptional activity using reporter assays. For this purpose, we transfected WT or $Rap1a^{-/-}$ hepatocytes with control or FoxO1-Gfp plasmids (Figures 6D and 6E, lower blots). We observed that the increase in *Igfbp1* and *G6pc* promoter activities upon FoxO1 overexpression was further upregulated in Rap1a-deficient hepatocytes (Figures 6D and 6E). We found

similar results upon forskolin and dexamethasone treatment, suggesting that FoxO1's transcriptional activity is increased in Rap1a-deficient cells (Figure S7J). To test the role of FoxO1 in Rap1a- and statin-mediated gluconeogenesis regulation, we silenced Rap1a in FoxO1,3,4-deficient hepatocytes. As above, Rap1a silenced hepatocytes expressed higher levels of *G6pc* and *Igfbp1* mRNAs than control hepatocytes, and in response to FoxO1,3,4 deficiency, this increment was abrogated, which supports the involvement of FoxO proteins in Rap1a-mediated gluconeogenic gene regulation (Figure 6F). Because nuclear localization of FoxO1 is required for its functional activity, we next measured nuclear FoxO1 levels in Rap1a-deficient or statin-treated hepatocytes. We observed that both Rap1a silencing and statin treatment increased nuclear FoxO1 without altering its total cellular levels (Figures 6G and 6H). One of the major upstream regulators of FoxO1's subcellular localization is insulin-receptor-signaling-activated serine/threonine kinase, Akt. Activation of Akt phosphorylates FoxO1, which results in FoxO1's cytoplasmic retention (Brunet et al., 1999). We then sought to determine if phosphorylation of FoxO1 or Akt was altered upon Rap1a deficiency. We found that Rap1a-silenced hepatocytes had significantly lower phospho-Akt and phospho-FoxO1 levels upon insulin stimulation or under basal conditions (Figures 6I and 6J). Similarly, rosuvastatin treatment of hepatocytes impaired insulin-induced Akt and FoxO1 phosphorylation (Figures 6K–6M). These results support the idea that statins or Rap1a inhibition reduce phosphorylation of Akt, which results in nuclear localization of FoxO1 and stimulation of gluconeogenesis.

Rap1a induces actin polymerization, and actin remodeling contributes to gluconeogenesis

We next sought to investigate possible mechanisms linking Rap1a activation to Akt-mediated FoxO1 regulation. Previous work in other cell types has demonstrated that Rap1a promotes filamentous actin (F-actin) polymerization (Mun and Jeon, 2012; Wang et al., 2017). As disruption of actin polymerization and cytoskeleton remodeling inhibits insulin-induced Akt activation (Lee et al., 2013; Peyrollier et al., 2000; Wang et al., 2012a), we considered the hypothesis that Rap1a may regulate gluconeogenesis through its effects on actin organization. We first examined whether Rap1a plays a role in actin polymerization in hepatocytes by staining F-actin filaments with Alexa Fluor 555-conjugated phalloidin in scrambled control or si-Rap1a–treated cells. We observed that si-Rap1a-treated hepatocytes had disrupted cytoskeletal structures as evidenced by short, fragmented F-actin filaments that coalesce to form cytoskeletal clumps (Figure 7A, see white arrows). This fragmented actin phenotype was similar to the actin phenotype of WT cells treated with the potent actin polymerization inhibitor cytochalasin D (Figure 7A), suggesting that Rap1a silencing results in dysregulation of actin cytoskeleton in hepatocytes. We next asked whether Rap1a inhibition induces gluconeogenesis via blocking actin polymerization. Consistent with this idea, we found that treatment of hepatocytes with different concentrations of cytochalasin D increased *G6pc* and *Pck1* mRNAs and resulted in a small but significant increase in glucose production (Figures 7B and 7C). We observed similar results when actin polymerization was inhibited using another actin polymerization inhibitor, latrunculin A (not shown). Conversely, treatment of primary hepatocytes with the actin filament polymerizing and stabilizing agent, jasplakinolide, lowered gluconeogenic gene expression and glucose production (Figures 7D and 7E). Similar to Rap1a inhibition, cytochalasin D was unable to induce *G6pc* and *Igfbp1* mRNAs in FoxO1,3,4-deficient hepatocytes (Figure 7F). Most

importantly, nuclear FoxO1 levels were increased, whereas insulin-stimulated phospho-Akt levels were decreased in cytochalasin D-treated hepatocytes (Figures 7G and 7H). Taken together, these data support the idea that hepatocyte Rap1a is involved in actin cytoskeleton dynamics, which contributes to the regulation of gluconeogenesis via Akt-mediated FoxO1 activation.

DISCUSSION

The combination of insulin resistance together with unopposed glucagon action results in increased HGP, which is largely responsible for the fasting hyperglycemia observed in obese patients with T2D (Gastaldelli et al., 2000; Unger and Cherrington, 2012). The most commonly used anti-diabetes therapy, metformin, is well-known for its ability to decrease hepatic gluconeogenesis, and other candidates that reduce HGP are being investigated as anti-glycemic agents (Kazda et al., 2016; Lee et al., 2021; Sharabi et al., 2017; Vella et al., 2019). Our results here identify the small GTPase Rap1a as a potential target that regulates HGP and glucose homeostasis. Mechanistically, we show that Rap1a stimulates actin polymerization, which regulates FoxO1's nuclear localization and activity. The role of FoxO1 in Rap1a action is supported by the finding that the stimulatory effects of Rap1a inhibition or actin depolymerization on gluconeogenesis are abrogated in FoxO1,3,4-deficient hepatocytes. With regard to FoxO1 regulation, we provide data that phosphorylation and activation of Akt, the major kinase that inhibits FoxO1 activity, are suppressed upon Rap1a deficiency. Of note, previous studies have implicated actin network and Rap1 in Akt activation through their effects on phosphoinositide 3-kinase (PI3K) activity, the upstream Akt regulator (Cahill et al., 2016; Eyster et al., 2005; Kortholt et al., 2010). Because of the importance of insulin receptor-Akt pathway in the pathogenesis of many obesity-associated metabolic dysfunctions, future investigations will be necessary to determine the molecular mechanisms linking Rap1a to Akt activation in hepatocytes.

In addition to obesity-induced hyperglycemia, our results show that inhibition of Rap1a activity or GGPP synthesis mediates elevated HGP in statin-treated hepatocytes and mice, which could be one of the underlying mechanisms linking statins to new-onset T2D. Interestingly, a recent work from another group independently reported that restoring geranylgeranyl isoprenoids improves statin-associated glucose intolerance in mice (Wang et al., 2022). *In vitro* findings from Wang et al. suggested that geranylgeranylation of another GTPase, Rab14, contributes to hepatic insulin signaling; however, the importance of Rab14 in statin-associated glucose intolerance was not studied. Given that rosuvastatin's ability to increase gluconeogenic genes was abolished in Rap1a deficient hepatocytes (Figures 4E and 4F), our results suggest that Rap1a inhibition is one of the major underlying mechanisms by which statins increase gluconeogenesis.

As all statins have high selectivity for the liver, largely because of efficient first-pass uptake (Schachter, 2005), the liver likely plays a major role in statin-induced glucose intolerance. However, statins may also contribute to glucose intolerance through their effects on other insulin-sensitive tissues and the pancreas. For example, statin treatment was shown to inhibit insulin secretion in a pancreatic β cell line (Salunkhe et al., 2016). Interestingly, a recent study in human subjects treated with atorvastatin for 10 weeks reported an increase in

steady-state plasma glucose without a decline in insulin secretion (Abbasi et al., 2021), yet the effect of long-term statin-use on β cell function remains to be investigated. It is important to note that activation of Epac2 and Rap1 in β cells is suggested to be beneficial in glucose homeostasis, as Epac2-Rap1 activation increases incretin-mediated insulin secretion (Takahashi et al., 2015). Regarding other possible non-hepatic effects, previous work showed impairment in insulin signaling in cultured adipocytes and myotubes upon statin treatment (Henriksbo et al., 2019; Hwang et al., 2019). Moreover, a recent study reported that GGPP and GGT1 are important regulators of brown adipocyte function and contribute to systemic glucose metabolism (Balaz et al., 2019). Future *in vivo* studies will be needed to determine whether geranylgeranylation or Rap1a in different cell types contribute to the statin-T2D link.

Clinical trials of PCSK9 inhibitors did not show an effect of these drugs on glycemia or T2D diagnosis; however, an increase in T2D risk has been observed in individuals with PCSK9 loss-of-function variants (Colhoun et al., 2016; Ference et al., 2016; Lotta et al., 2016; Sabatine et al., 2017; Sattar et al., 2017; Schmidt et al., 2017). On the other hand, LDL-modulating allele in *APOB* showed no relationship with diabetes risk (Xu et al., 2017). Thus, the T2D link with statins and PCSK9 loss-of-function variants is complex and may not be simply attributed to their effects on liver LDLR expression or plasma LDL, which is in line with our data showing that intracellular cholesterol or LDLR do not impact statin-induced gluconeogenesis in hepatocytes. Finally, while our results have defined an important mechanism that may underlie statins' hyperglycemic effects, it is important to note that the benefits of statin use for the reduction of cardiovascular disease risk outweigh the risk of developing T2D in the majority of patients, especially in individuals with higher cardiovascular disease risk (Mach et al., 2018; Sattar et al., 2014).

Limitations of the study

The data presented in this study demonstrate that Rap1a suppresses gluconeogenesis and inhibits the aberrant activation of HGP. As increased gluconeogenesis is a common feature of both fasting and obesity, we observed lower active-Rap1a levels in transition from fed to fasting state or in obese mice liver. However, we did not identify the upstream molecular mediators governing this regulation. Our data also suggest that hepatic Rap1a inhibition, through lowering intracellular GGPP isoprenoid levels, is a major mechanism by which statins increase gluconeogenesis and cause hyperglycemia. In this regard, one limitation of our study is that we did not evaluate the effects of statins and GGOH treatment on other insulin-sensitive tissues, an area that should be investigated using the hyperinsulinemic-euglycemic clamp studies. Finally, the mechanisms by which Rap1a and actin cytoskeleton organization regulate Akt-mediated FoxO1 activity remain to be determined.

STAR★METHODS

RESOURCE AVAILABILITY

Lead contact—Further information and requests for resources and reagents should be directed to and will be fulfilled by the lead contact, Dr. Lale Ozcan (lo2192@cumc.columbia.edu).

Materials availability—This study did not generate new unique reagents.

Data and code availability

- All data reported in this paper will be shared by the lead contact upon request.
- This paper does not report original code.
- Any additional information required to reanalyze the data reported in this paper is available from the lead contact upon request.

EXPERIMENTAL MODEL AND SUBJECT DETAILS

Animal models—WT C57BL/6J (stock number: 000664), *db/db* and *db*/+ (stock number: 000697) and diet-induced obese (DIO, stock number: 380050) mice and their controls (stock number: 380056) were from Jackson Labs. *Foxo1,3,4*$^{fl/fl}$ mice were generously provided by Dr. Rebecca Haeusler from Columbia University (Haeusler et al., 2010). *Rap1a*$^{fl/fl}$ mice were generated by crossbreeding *Rap1ab* double floxed mice (Jackson Labs, stock number: 021066) with WT C57BL/6J mice and confirmed by genotyping. For all experiments, twelve- to thirty-three-week-old male mice with similar weight were randomly assigned to experimental and control groups. The mice were housed in standard cages at 22°C under a 12-12-hour light-dark cycle in a barrier facility with ad libitum access to water and food. Animal studies were performed in accordance with the Columbia University Institutional Animal Care and Use Committee.

Human liver samples and human primary hepatocytes—Part of the human liver samples were obtained from the NIH-supported Liver Tissue Cell Distribution System at the University of Minnesota. The samples were collected postmortem on the date of liver transplantation and preserved as frozen samples. Part of the human liver samples were obtained from patients undergoing bariatric surgery or clinically indicated laparoscopic procedures at the New York Presbyterian Hospital, Columbia University Irving Medical Center. Samples were obtained from intra-operative needle biopsies of the liver at a standard anatomic location. The biopsy specimens were frozen immediately in liquid nitrogen and stored at −80°C until subsequent analyses. The mean age of the donors was 50 (ranging from 32 to 68 years old), and the donors included 4 males and 8 females, as noted in the figures. The Institutional Review Board at the Columbia University Medical Center approved the research protocol. All participants provided written informed consent.

Metabolism-qualified human plateable hepatocytes from a fifty-three-year-old male donor (ThermoFisher, cat # HMCPMS, lot # HU8272) was thawed using cryopreserved hepatocyte recovery medium (ThermoFisher, cat # CM7000) and cultured in Williams' Medium E (ThermoFisher, cat # A1217601) containing hepatocyte maintenance supplement pack (ThermoFisher, cat # CM4000). The cells were grown at 37°C and 5% CO_2 and treated as noted in the figure legends.

Primary mouse hepatocytes—Primary mouse hepatocytes were isolated from 8- to 14-week-old male or female mice as described previously (Ozcan et al., 2012). Briefly, after the mice were euthanized and their abdomens were opened, a catheter was placed

into the inferior vena cava. The liver was first perfused with Hanks' balanced salt solution followed by perfusion with a collagenase solution (Sigma-Aldrich, cat # C2674). The liver was forceps-disaggregated, and the digested liver was centrifuged at 50 × g for 5 min. The supernatant fraction was removed, and the hepatocytes in the pellet were resuspended and cultured in DMEM/F12 (ThermoFisher, cat # 11320) containing 10% (vol/vol) heat-inactivated FBS (ThermoFisher, cat # 16140–071) and 1% penicillin-streptomycin solution (Corning, cat # 30-002-Cl). All cells were grown at 37°C and 5% CO_2.

Cell lines—AML-12 (alpha mouse liver 12) mouse hepatocyte cells were obtained from ATCC (cat # CRL-2254). Cells were cultured in DMEM/F12 medium (ThermoFisher, cat # 11320) with 10% (vol/vol) heat-inactivated FBS (ThermoFisher, cat # 16140–071) and 1% penicillin-streptomycin solution (Corning, cat #30-002-Cl) and grown at 37°C and 5% CO_2. No authentication was done on AML-12 cells by the authors as the experiments were performed in cells cultured for less than 10 passages.

METHOD DETAILS

Reagents and antibodies—Forskolin (cat # F6886), dexamethasone (cat # D4902), GGT1i (cat # G5294 and G5169), FTi (cat # F9803), Fluvastatin (cat # SML0038), glucose (cat # G7021), glucagon (cat # G2044) and insulin (cat # I0516) were from Sigma-Aldrich. Simvastatin for cell treatment was from Sigma-Aldrich (cat # S6196) and simvastatin for mouse experiments was from Tokyo Chemical Industry (TCI) Company (cat # S0509). Rosuvastatin (cat # 18813), GGPP (cat # 63330) and GGOH (cat # 13272) were from Cayman Chemicals. Anti-β-actin (cat # 4970), anti-pan-Cadherin (cat # 4068), anti-GFP (cat # 2956), anti-GAPDH (cat # 5174), anti-p-Akt (cat # 4060), anti-Akt (cat # 4691), anti-FoxO1 (cat # 2880), anti-p-FoxO1 (cat # 9464), anti-Lamin A/C (cat # 4777), anti-nucleophosmin (cat # 3542), anti-p-CREB (cat # 9198), anti-CREB (cat # 9197), anti-p-PKA substrates (cat # 9624) and anti-Hsp90 (cat # 4877) antibodies were from Cell Signaling Technology. Anti-Rap1a antibody (cat # AF3767) was from R&D Systems. Anti-Na,K-ATPase antibody (cat # ab76020) was from Abcam. siRNAs were purchased from Integrated DNA Technologies and designed as following: siEpac2, 5'-rArArGrCrArArCrArGrArUrUrCrGrGrUrUrUrUrArArArUGA-3' (sense), 5'-rUrCrArUrUrUrArArArArArCrCrGrArArUrCrUrGrUrUrGrCrUrUrCrA-3' (antisense), siRap1a, 5'-rCrArArGrCrUrArGrUrArGrUrCrCrUrUrGrGrUrUrCrArGGA-3' (sense), 5'-rUrCrCrUrGrArArCrCrArArGrGrArCrUrArCrUrArGrCrUrUrGrUrA-3' (antisense), siPggt1b, 5'-rCrUrUrArArGrGrUrGrUrGrCrCrArArCrUrArArArCrArUGT-3' (sense), 5'-rArCrArUrGrUrUrUrArGrUrUrGrGrCrArCrArCrCrUrUrArArGrGrArA-3′ (antisense). AAV8-TBG-Cre and AAV8-TBG-Gfp were obtained from Gene Therapy Resource Program (GTRP) of NHLBI or purchased from Addgene (cat # 105535-AAV8 and # 107787-AAV8). Adeno-associated virus subtype 8 (AAV8)-shRNA targeting murine Pggt1b was made by annealing complementary oligonucleotides 5′-CACCAAAGCCATCAGCTACATTAGAAGAAGTCAAGAGCTTCTTCTAATGTAGCTGATGGCTT-3′), which were then ligated into the self-complementary AAV8-RSV-GFP-H1 vector as described previously (Lisowski et al., 2014). The resultant constructs were amplified by Salk Institute Gene Transfer, Targeting, and Therapeutics Core. AAV8-TBG-CA-Rap1a was from Penn Vector Core. Rap1-E63 (CA-Rap1a) plasmid was described

previously (Lafuente et al., 2004) (Addgene, cat # 32698) and amplified by Genewiz. Adenoviruses encoding LacZ and CA-Rap1a were described previously (Wittchen et al., 2011) and amplified by Viraquest, Inc. (North Liberty, IA).

Mouse treatments and metabolic experiments—Four-week-old male *Rap1a*$^{fl/fl}$ mice were fed with a high-fat diet with 60% kcal from fat (Research Diets, cat # D12492) for 12–20 weeks. The mice were injected with adeno-associated virus (AAV) expressing Cre recombinase, driven by the thyroxin-binding globulin (TBG) promoter (AAV8-TBG-Cre) to obtain hepatocyte-specific Rap1a deficient mice. Littermates injected with AAV8-TBG-Gfp were used as control mice. AAV8-H1-scrambled RNA (control), AAV8-H1-shPggt1b, AAV8-TBG-CA-Rap1a, AAV8-TBG-Gfp (control), adeno-CA-Rap1a and adeno-LacZ (control) viruses were delivered by tail vein injections of eighteen-week-old male DIO mice or six-week-old male *db/db* mice at a dose of 1–2.5 × 10^{11} genome copies per mouse for AAV and 0.5–0.75 × 10^{9} plaque-forming units per mouse for adenoviruses. For statin treatment experiments, 18-week-old male DIO mice (Jackson Labs, stock number: 380050) were fed a high-fat diet containing 0.02% (w/w) simvastatin (Research Diets, cat #D12492) for 12 weeks. Geranylgeraniol (GGOH) was given by oral gavage at a dose of 100 mg/kg/day for 3 weeks.

Fasting blood glucose was measured in mice that were fasted for 5 h or overnight, with free access to water, using a glucose meter (OneTouch Ultra). Plasma insulin levels were measured in mice that were fasted for 5 h or overnight using ultrasensitive mouse insulin ELISA Kit (Crystal Chem, cat # 90080). Glucose tolerance tests (GTT) were performed in overnight-fasted mice by assaying blood glucose at various times after intraperitoneal injection of glucose (0.5 g/kg for *db/db* mice and 1.0–1.5 g/kg for DIO mice).

siRNA and plasmid transfections—Transfections with siRNA or plasmids were carried out using Lipofectamine RNAiMAX or Lipofectamine 3000 reagents (ThermoFisher, cat # 13-778-150 and # L3000015) according to manufacturer's instructions. After incubating the cells with siRNA or plasmids for 5 h, the media were changed to DMEM/F12 medium with 10% (vol/vol) heat-inactivated FBS and 1% penicillin-streptomycin solution, and the cells were incubated for an additional 48–60 h.

Gluconeogenesis and glucose production—For gluconeogenesis, the hepatocytes were serum-depleted overnight by incubation in medium containing 0.5% FBS and were then incubated in serum-free media containing 10 μM forskolin plus 100 nM dexamethasone (F + D) or 100 nM glucagon for three hours. For glucose production assays, primary hepatocytes were cultured in regular DMEM-F12 medium. Cells were then washed three times with PBS and incubated with glucose-free DMEM-F12 without phenol red media containing 2 mM sodium pyruvate, 20 mM lactate, 100 nM dexamethasone, and 10 μM forskolin plus 100 nM dexamethasone for sixteen hours. Culture media was collected, and the cells were washed with PBS and lysed in RIPA buffer for protein concentration determination. Glucose concentration in the medium was measured using Glucose (GO) Assay Kit (Sigma-Aldrich, cat # GAGO20) and normalized to the protein amount of the cells. The data is presented as relative to control.

Immunoblotting—Total liver or cell protein was lysed using RIPA buffer (Thermo Scientific, cat # PI89901) containing 2 mM PMSF, 5 μg/mL leupeptin, 10 nM okadaic acid and 5 μg/mL aprotinin on ice. Protein concentration was measured. Protein extracts were electrophoresed on SDS-polyacrylamide gels and transferred to 0.45 μm or 0.2 μm PVDF membranes. Blots were blocked in Tris-buffered saline with 0.1% Tween 20 containing 5% BSA at room temperature for one hour. Membranes were then incubated overnight at 4°C with primary antibodies. The protein bands were detected with horseradish peroxidase-conjugated secondary antibodies and Supersignal West Pico enhanced chemiluminescent solution (ThermoFisher, cat# 34580). ImageJ was used for densitometric analysis of the immunoblots.

Membrane protein extraction—Membrane proteins were isolated as described previously (Petersen et al., 2016). Briefly, sells were washed with cold HBSS and lysed with buffer A containing 20 mM Tris-HCl pH7.4, 1 mM EDTA, 0.25 mM EGTA, 250 mM Sucrose, 10 mM NaF, and 2 mM Na_3VO_4 on ice. Cell lysates were collected and centrifuged at 500 × g for 10 min at 4°C. The supernatant was collected and centrifuged at 100,000 × rpm for 1 h at 4°C. Supernatant was discarded, and the pellet was re-suspended with buffer B containing 250 mM Tri-HCl pH7.4, 1 mM EDTA, 0.25 mM EGTA, 10 mM NaF, 2 mM Na_3VO_4 and 2% Triton X- on ice for 30 min. Lysates were centrifuged at 15,000 × rpm for 20 min at 4°C. Supernatant was collected, and protein concentration was measured.

Nuclear protein extraction—A modified Active Motif Nuclear Kit (cat # 40010) was used for nuclear protein extraction. Cells were scraped with cold PBS containing 2 mM PMSF, 5 μg/mL leupeptin, 10 nM okadaic acid and centrifuged at 200 × g for 5 min at 4°C. Supernatant was discarded, and the pellet was re-suspended with 1X hypotonic buffer and incubated on ice for 15 min followed by detergent treatment. The lysates were then centrifuged at 14,000 × g for 30 s at 4°C. Supernatant was discarded, and the pellet was re-suspended in RIPA buffer containing 2 mM PMSF, 5 μg/mL leupeptin, 10 nM okadaic acid and 5 μg/mL aprotinin for 30 min on ice. Lysates were centrifuged at 14,000 × g for 10 min at 4°C, and the supernatant was collected, and protein concentration was measured.

Rap1a activity assay—Rap1a activity was assayed using Active Rap1 Detection Kit (Cell Signaling Technology, cat # 8818). Cells were washed with cold PBS and lysed with lysis/binding/washing buffer containing 2 mM PMSF, 5 μg/mL leupeptin, 10 nM okadaic acid and 5 μg/mL aprotinin. GST-RalGDS-RBD fusion protein was used to bind the activated form of GTP-bound Rap1, which was then immunoprecipitated with glutathione resin. Rap1a activation levels were determined by western blot using a Rap1a primary antibody.

Measurement of cAMP—Cyclic AMP XP® Assay Kit (Cell Signaling Technology, cat # 4339) was used for cAMP measurements. Cells were lysed with lysis buffer and centrifuged briefly to remove cell debris. Clear lysates were transferred to the cAMP rabbit monoclonal antibody-coated microwells, mixed with HRP-linked cAMP solution, and incubated at room temperature for 3 h. Following washing to remove excess sample cAMP and HRP-linked cAMP, HRP substrate TMB is added to develop color and then absorbance was measured.

Transcriptional reporter assays—Hepatocytes were transfected with Igfbp1-promoter/pGL3 (Addgene, cat # 12146) and Gfp-FoxO1 plasmids (Addgene, cat # 17551), and renilla luciferase vector was co-transfected as an internal control (Addgene, cat # 27163) (Chen and Prywes, 1999; Frescas et al., 2005; Nakae et al., 2000). Cells were collected 72 h post-transfection with 1X Passive Lysis Buffer (Promega, cat # E1910). Firefly luciferase reporter was determined by addition of Luciferase Assay Substrate and quantification of luminescence on a FLUOstar Omega plate reader.

Preparation of cholesterol rich liposomes—DMPC (1,2-dimyristoyl-sn-glycero-3-phosphocholine, Avanti Polar Lipids, cat # 850345) and cholesterol (Sigma-Aldrich, cat # C8667) were dissolved in chloroform. For cholesterol rich liposomes, 40 mg of DMPC was mixed with 80 mg of cholesterol in a glass vessel and the solvent was dried under a stream of nitrogen gas. Multilamellar vesicles (large liposomes>1uM) were formed by addition of 10 mL of PBS to the lipid film and then shaking the mixture. The liposomes were reduced in size by probe sonication on ice for 10–15 min. The solution turned white and was centrifuged at 10,000 × g for 10 min. Supernatant was collected and extruded through 100 nm polycarbonate filter. Aliquots were stored in glass vials under argon at 4°C and used within 2 weeks.

Phalloidin staining—Hepatocytes cultured in glass coverslips were washed with PBS and fixed with 4% formaldehyde for 20 min at room temperature. The cells were then permeabilized with 0.1% Triton X-100 in PBS for 5 min, followed by 3 washes of PBS. F-actin fibers were stained for 1 h at room temperature with Phalloidin-iFluor 488 reagent (Abcam, cat # ab176753, 1:1000 diluted in 1%BSA). After washing three times with PBS, images were taken using a Leica epifluorescence microscope (DMI6000B).

Quantitative PCR—RNA was extracted from hepatocytes or liver tissue using TRI Reagent (Sigma-Aldrich, cat # T9424) and cDNA was synthesized from 1 ug of RNA using a cDNA synthesis kit (Invitrogen). Real-time PCR was performed using a 7500 Real-Time PCR system and SYBR Green reagents (Applied Biosystems). The primer sequences are listed in Table S1.

QUANTIFICATION AND STATISTICAL ANALYSIS

All results are presented as mean ± SEM. Statistical significance was determined using SigmaPlot software. Data that passed the normality tests were analyzed using Student's t-test and ANOVA. Data that were not normally distributed were analyzed using the nonparametric Mann-Whitney U test. Differences were considered statistically significant at $p < 0.05$.

Supplementary Material

Refer to Web version on PubMed Central for supplementary material.

ACKNOWLEDGMENTS

We thank Dr. Rebecca Haeusler (Columbia University) for *Foxo1,3,4*$^{fl/fl}$ mice and Dr. Keith Burridge and Dr. Erika Wittchen (University of North Carolina at Chapel Hill) for CA-Rap1a adenovirus. We would like to acknowledge the Gene Therapy Resource Program (GTRP) of the NHLBI for providing AAV8-TBG-Cre and AAV8-TBG-Gfp, and NIH-supported Liver Tissue Cell Distribution System at the University of Minnesota for arranging and providing de-identified human liver samples (NIH Contract # HSN276201200017C). This work was supported by State Scholarship Fund from China Scholarship Council (201906370237) to Y.W.; Medical Student Research Training Grant (2T32DK007559-27A1) to J.A.Z.; NIH grant (DK124457) and Russell Berrie Foundation Pre-translational Diabetes Research Award to L.O.

REFERENCES

Abbasi F, Lamendola C, Harris CS, Harris V, Tsai MS, Tripathi P, Abbas F, Reaven GM, Reaven PD, Snyder MP, et al. (2021). Statins are associated with increased insulin resistance and secretion. Arterioscler. Thromb. Vasc. Biol 41, 2786–2797. 10.1161/ATVBAHA.121.316159. [PubMed: 34433298]

Baigent C, Keech A, Kearney PM, Blackwell L, Buck G, Pollicino C, Kirby A, Sourjina T, Peto R, Collins R, et al. (2005). Efficacy and safety of cholesterol-lowering treatment: prospective meta-analysis of data from 90, 056 participants in 14 randomised trials of statins. Lancet 366, 1267–1278. 10.1016/S0140-6736(05)67394-1. [PubMed: 16214597]

Balaz M, Becker AS, Balazova L, Straub L, Müller J, Gashi G, Maushart CI, Sun W, Dong H, Moser C, et al. (2019). Inhibition of mevalonate pathway prevents adipocyte browning in mice and men by affecting protein prenylation. Cell Metab. 29, 901–916.e8. 10.1016/j.cmet.2018.11.017. [PubMed: 30581121]

Benjamin EJ, Virani SS, Callaway CW, Chamberlain AM, Chang AR, Cheng S, Chiuve SE, Cushman M, Delling FN, Deo R, et al. (2018). Heart disease and stroke statistics-2018 update: a report from the American heart association. Circulation 137, e67–e492. 10.1161/CIR.0000000000000558. [PubMed: 29386200]

Bos JL, Rehmann H, and Wittinghofer A (2007). GEFs and GAPs: critical elements in the control of small G proteins. Cell 129, 865–877. 10.1016/j.cell.2007.05.018. [PubMed: 17540168]

Brunet A, Bonni A, Zigmond MJ, Lin MZ, Juo P, Hu LS, Anderson MJ, Arden KC, Blenis J, and Greenberg ME (1999). Akt promotes cell survival by phosphorylating and inhibiting a Forkhead transcription factor. Cell 96, 857–868. 10.1016/s0092-8674(00)80595-4. [PubMed: 10102273]

Cahill ME, Bagot RC, Gancarz AM, Walker DM, Sun H, Wang ZJ, Heller EA, Feng J, Kennedy PJ, Koo JW, et al. (2016). Bidirectional synaptic structural plasticity after chronic cocaine administration occurs through Rap1 small GTPase signaling. Neuron 89, 566–582. 10.1016/j.neuron.2016.01.031. [PubMed: 26844834]

Casula M, Mozzanica F, Scotti L, Tragni E, Pirillo A, Corrao G, and Catapano AL (2017). Statin use and risk of new-onset diabetes: a meta-analysis of observational studies. Nutr. Metab. Cardiovasc. Dis 27, 396–406. 10.1016/j.numecd.2017.03.001. [PubMed: 28416099]

Cederberg H, Stančáková A, Yaluri N, Modi S, Kuusisto J, and Laakso M (2015). Increased risk of diabetes with statin treatment is associated with impaired insulin sensitivity and insulin secretion: a 6 year follow-up study of the METSIM cohort. Diabetologia 58, 1109–1117. 10.1007/s00125-015-3528-5.. [PubMed: 25754552]

Chen X, and Prywes R (1999). Serum-induced expression of the cdc25A gene by relief of E2F-mediated repression. Mol. Cell Biol 19, 4695–4702. 10.1128/MCB.19.7.4695. [PubMed: 10373518]

Chrivia JC, Kwok RP, Lamb N, Hagiwara M, Montminy MR, and Goodman RH (1993). Phosphorylated CREB binds specifically to the nuclear protein CBP. Nature 365, 855–859. 10.1038/365855a0. [PubMed: 8413673]

Colhoun HM, Ginsberg HN, Robinson JG, Leiter LA, Müller-Wieland D, Henry RR, Cariou B, Baccara-Dinet MT, Pordy R, Merlet L, and Eckel RH (2016). No effect of PCSK9 inhibitor alirocumab on the incidence of diabetes in a pooled analysis from 10 ODYSSEY Phase 3 studies. Eur. Heart J 37, 2981–2989. 10.1093/eurheartj/ehw292. [PubMed: 27460890]

Crandall JP, Mather K, Rajpathak SN, Goldberg RB, Watson K, Foo S, Ratner R, Barrett-Connor E, and Temprosa M (2017). Statin use and risk of developing diabetes: results from the Diabetes Prevention Program. BMJ Open Diabetes Res. Care 5, e000438. 10.1136/bmjdrc-2017-000438.

Eyster CA, Duggins QS, and Olson AL (2005). Expression of constitutively active Akt/protein kinase B signals GLUT4 translocation in the absence of an intact actin cytoskeleton. J. Biol. Chem 280, 17978–17985. 10.1074/jbc.M409806200.. [PubMed: 15738003]

FDA(2012). Drug Safety Communication Drug Safety Communication. https://www.fda.gov/drugs/drugsafety/ucm293101.htm.

Ference BA, Robinson JG, Brook RD, Catapano AL, Chapman MJ, Neff DR, Voros S, Giugliano RP, Davey Smith G, Fazio S, and Sabatine MS (2016). Variation in PCSK9 and HMGCR and risk of cardiovascular disease and diabetes. N. Engl. J. Med 375, 2144–2153. 10.1056/NEJMoa1604304. [PubMed: 27959767]

Frescas D, Valenti L, and Accili D (2005). Nuclear trapping of the forkhead transcription factor FoxO1 via Sirt-dependent deacetylation promotes expression of glucogenetic genes. J. Biol. Chem 280, 20589–20595. 10.1074/jbc.M412357200. [PubMed: 15788402]

Gastaldelli A, Baldi S, Pettiti M, Toschi E, Camastra S, Natali A, Landau BR, and Ferrannini E (2000). Influence of obesity and type 2 diabeteson gluconeogenesis and glucose output in humans: a quantitative study. Diabetes 49, 1367–1373. 10.2337/diabetes.49.8.1367. [PubMed: 10923639]

Ghomashchi F, Zhang X, Liu L, and Gelb MH (1995). Binding of prenylated and polybasic peptides to membranes: affinities and intervesicle exchange. Biochemistry 34, 11910–11918. 10.1021/bi00037a032. [PubMed: 7547927]

Gibbs BS, Zahn TJ, Mu Y, Sebolt-Leopold JS, and Gibbs RA (1999). Novel farnesol and geranylgeraniol analogues: a potential new class of anticancer agents directed against protein prenylation. J. Med. Chem 42, 3800–3808. 10.1021/jm9902786. [PubMed: 10508429]

Gloerich M, and Bos JL (2011). Regulating Rap small G-proteins in time and space. Trends Cell Biol. 21, 615–623. 10.1016/j.tcb.2011.07.001. [PubMed: 21820312]

Goldstein JL, and Brown MS (2009). The LDL receptor. Arterioscler. Thromb. Vasc. Biol 29, 431–438. 10.1161/atvbaha.108.179564. [PubMed: 19299327]

Goldstein JL, and Brown MS (2015). A century of cholesterol and coronaries: from plaques to genes to statins. Cell 161, 161–172. 10.1016/j.cell.2015.01.036. [PubMed: 25815993]

Goody RS, Müller MP, and Wu YW (2017). Mechanisms of action of Rab proteins, key regulators of intracellular vesicular transport. Biol. Chem 398, 565–575. 10.1515/hsz-2016-0274. [PubMed: 27845878]

Haeusler RA, Hartil K, Vaitheesvaran B, Arrieta-Cruz I, Knight CM, Cook JR, Kammoun HL, Febbraio MA, Gutierrez-Juarez R, Kurland IJ, and Accili D (2014). Integrated control of hepatic lipogenesis versus glucose production requires FoxO transcription factors. Nat. Commun 5, 5190. 10.1038/ncomms6190. [PubMed: 25307742]

Haeusler RA, Kaestner KH, and Accili D (2010). FoxOs function synergistically to promote glucose production. J. Biol. Chem 285, 35245–35248. 10.1074/jbc.C110.175851. [PubMed: 20880840]

Henriksbo BD, Tamrakar AK, Xu J, Duggan BM, Cavallari JF, Phulka J, Stampfli MR, Ashkar AA, and Schertzer JD (2019). Statins promote interleukin-1beta-dependent adipocyte insulin resistance through lower prenylation, not cholesterol. Diabetes 68, 1441–1448. 10.2337/db18-0999. [PubMed: 31010959]

Herzig S, Long F, Jhala US, Hedrick S, Quinn R, Bauer A, Rudolph D, Schutz G, Yoon C, Puigserver P, et al. (2001). CREB regulates hepatic gluconeogenesis through the coactivator PGC-1. Nature 413, 179–183. 10.1038/35093131. [PubMed: 11557984]

Hwang JH, Kim AR, Kim KM, Il Park J, Oh HT, Moon SA, Byun MR, Jeong H, Kim HK, Yaffe MB, et al. (2019). TAZ couples Hippo/Wnt signalling and insulin sensitivity through Irs1 expression. Nat. Commun 10, 421. 10.1038/s41467-019-08287-x. [PubMed: 30679431]

Hwang JY, Sim X, Wu Y, Liang J, Tabara Y, Hu C, Hara K, Tam CHT, Cai Q, Zhao Q, et al. (2015). Genome-wide association meta-analysis identifies novel variants associated with fasting plasma glucose in East Asians. Diabetes 64, 291–298. 10.2337/db14-0563. [PubMed: 25187374]

Jaśkiewicz A, Pająk B, and Orzechowski A (2018). The many faces of Rap1 GTPase. Int. J. Mol. Sci 19, E2848. 10.3390/ijms19102848. [PubMed: 30241315]

Jaśkiewicz A, Pająk B, Litwiniuk A, Urbańska K, and Orzechowski A (2018). Geranylgeraniol prevents statin-dependent myotoxicity in C2C12 muscle cells through RAP1 GTPase prenylation and cytoprotective autophagy. Oxid. Med. Cell. Longev 2018, 6463807. 10.1155/2018/6463807. [PubMed: 29951166]

Kazda CM, Ding Y, Kelly RP, Garhyan P, Shi C, Lim CN, Fu H, Watson DE, Lewin AJ, Landschulz WH, et al. (2016). Evaluation of efficacy and safety of the glucagon receptor antagonist LY2409021 in patients with type 2 diabetes: 12- and 24-week phase 2 studies. Diabetes Care 39, 1241–1249. 10.2337/dc15-1643. [PubMed: 26681715]

Kitayama H, Sugimoto Y, Matsuzaki T, Ikawa Y, and Noda M (1989). A ras-related gene with transformation suppressor activity. Cell 56, 77–84. [PubMed: 2642744]

Kortholt A, Bolourani P, Rehmann H, Keizer-Gunnink I, Weeks G, Wittinghofer A, and Van Haastert PJM (2010). A Rap/phosphatidylinositol 3-kinase pathway controls pseudopod formation [corrected]. Mol. Biol. Cell 21, 936–945. 10.1091/mbc.E09-03-0177. [PubMed: 20089846]

Lafuente EM, van Puijenbroek AAFL, Krause M, Carman CV, Freeman GJ, Berezovskaya A, Constantine E, Springer TA, Gertler FB, and Boussiotis VA (2004). RIAM, an Ena/VASP and Profilin ligand, interacts with Rap1-GTP and mediates Rap1-induced adhesion. Dev. Cell 7, 585–595. 10.1016/j.devcel.2004.07.021. [PubMed: 15469846]

Langlet F, Haeusler RA, Lindén D, Ericson E, Norris T, Johansson A, Cook JR, Aizawa K, Wang L, Buettner C, and Accili D (2017). Selective inhibition of FOXO1 activator/repressor balance modulates hepatic glucose handling. Cell 171, 824–835.e18. 10.1016/j.cell.2017.09.045. [PubMed: 29056338]

Lee A, Hakuno F, Northcott P, Pessin JE, and Rozakis Adcock M (2013). Nexilin, a cardiomyopathy-associated F-actin binding protein, binds and regulates IRS1 signaling in skeletal muscle cells. PLoS One 8, e55634. 10.1371/journal.pone.0055634. [PubMed: 23383252]

Lee YK, Diaz B, Deroose M, Lee SX, Belvedere S, Accili D, Leibel RL, and Lin HV (2021). FOXO1 inhibition synergizes with FGF21 to normalize glucose control in diabetic mice. Mol. Metab 49, 101187. 10.1016/j.molmet.2021.101187. [PubMed: 33577983]

Lin HV, and Accili D (2011). Hormonal regulation of hepatic glucose production in health and disease. Cell Metab. 14, 9–19. 10.1016/j.cmet.2011.06.003. [PubMed: 21723500]

Lisowski L, Dane AP, Chu K, Zhang Y, Cunningham SC, Wilson EM, Nygaard S, Grompe M, Alexander IE, and Kay MA (2014). Selection and evaluation of clinically relevant AAV variants in a xenograft liver model. Nature 506, 382–386. 10.1038/nature12875. [PubMed: 24390344]

Lotta LA, Sharp SJ, Burgess S, Perry JRB, Stewart ID, Willems SM, Luan J, Ardanaz E, Arriola L, Balkau B, et al. (2016). Association between low-density lipoprotein cholesterol-lowering geneticvariants and risk of type 2 diabetes: a meta-analysis. JAMA 316, 1383–1391. 10.1001/jama.2016.14568. [PubMed: 27701660]

Mach F, Ray KK, Wiklund O, Corsini A, Catapano AL, Bruckert E, De Backer G, Hegele RA, Hovingh GK, Jacobson TA, et al. (2018). Adverse effects of statin therapy: perception vs. the evidence - focus on glucose homeostasis, cognitive, renal and hepatic function, haemorrhagic stroke and cataract. Eur. Heart J 39, 2526–2539. 10.1093/eurheartj/ehy182. [PubMed: 29718253]

Magnusson I, Rothman DL, Katz LD, Shulman RG, and Shulman GI (1992). Increased rate of gluconeogenesis in type II diabetes mellitus. A 13C nuclear magnetic resonance study. J. Clin. Invest 90, 1323–1327. 10.1172/JCI115997. [PubMed: 1401068]

Manganiello V, and Vaughan M (1972). An effect of dexamethasone on adenosine 3', 5'-monophosphate content and adenosine 3', 5'-monophosphate phosphodiesterase activity of cultured hepatoma cells. J. Clin. Invest 51, 2763–2767. 10.1172/JCI107096. [PubMed: 4341439]

Matsumoto M, Han S, Kitamura T, and Accili D (2006). Dual role of transcription factor FoxO1 in controlling hepatic insulin sensitivity and lipid metabolism. J. Clin. Invest 116, 2464–2472. 10.1172/JCI27047. [PubMed: 16906224]

Mun H, and Jeon TJ (2012). Regulation of actin cytoskeleton by Rap1 binding to RacGEF1. Mol. Cells 34, 71–76. 10.1007/s10059-012-0097-z. [PubMed: 22644079]

Nakae J, Barr V, and Accili D (2000). Differential regulation of gene expression by insulin and IGF-1 receptors correlates with phosphorylation of a single amino acid residue in the forkhead transcription factor FKHR. EMBO J. 19, 989–996. 10.1093/emboj/19.5.989. [PubMed: 10698940]

Ozcan L, Wong CCL, Li G, Xu T, Pajvani U, Park SKR, Wronska A, Chen BX, Marks AR, Fukamizu A, et al. (2012). Calcium signaling through CaMKII regulates hepatic glucose production in fasting and obesity. Cell Metab. 15, 739–751. 10.1016/j.cmet.2012.03.002. [PubMed: 22503562]

Pajvani UB, and Accili D (2015). The new biology of diabetes. Diabetologia 58, 2459–2468. 10.1007/s00125-015-3722-5. [PubMed: 26248647]

Petersen MC, Madiraju AK, Gassaway BM, Marcel M, Nasiri AR, Butrico G, Marcucci MJ, Zhang D, Abulizi A, Zhang XM, et al. (2016). Insulin receptor Thr1160 phosphorylation mediates lipid-induced hepatic insulin resistance. J. Clin. Invest 126, 4361–4371. 10.1172/JCI86013. [PubMed: 27760050]

Petersen MC, Vatner DF, and Shulman GI (2017). Regulation of hepatic glucose metabolism in health and disease. Nat. Rev. Endocrinol 13, 572–587. 10.1038/nrendo.2017.80. [PubMed: 28731034]

Peyrollier K, Hajduch E, Gray A, Litherland GJ, Prescott AR, Leslie NR, and Hundal HS (2000). A role for the actin cytoskeleton in the hormonal and growth-factor-mediated activation of protein kinase B. Biochem. J 352 Pt 3, 617–622. [PubMed: 11104665]

Preiss D, Seshasai SRK, Welsh P, Murphy SA, Ho JE, Waters DD, DeMicco DA, Barter P, Cannon CP, Sabatine MS, et al. (2011). Risk of incident diabetes with intensive-dose compared with moderate-dose statin therapy: a meta-analysis. JAMA 305, 2556–2564. 10.1001/jama.2011.860. [PubMed: 21693744]

Ramnanan CJ, Edgerton DS, Kraft G, and Cherrington AD (2011). Physiologic action of glucagon on liver glucose metabolism. Diabetes Obes. Metab 13, 118–125. 10.1111/j.1463-1326.2011.01454.x.

Ridker PM, Danielson E, Fonseca FAH, Genest J, Gotto AM Jr., Kastelein JJP, Koenig W, Libby P, Lorenzatti AJ, MacFadyen JG, et al. (2008). Rosuvastatin to prevent vascular events in men and women with elevated C-reactive protein. N. Engl. J. Med 359, 2195–2207. 10.1056/NEJMoa0807646. [PubMed: 18997196]

Sabatine MS, Leiter LA, Wiviott SD, Giugliano RP, Deedwania P, De Ferrari GM, Murphy SA, Kuder JF, Gouni-Berthold I, Lewis BS, et al. (2017). Cardiovascular safety and efficacy of the PCSK9 inhibitor evolocumab in patients with and without diabetes and the effect of evolocumab on glycaemia and risk of new-onset diabetes: a prespecified analysis of the FOURIER randomised controlled trial. Lancet Diabetes Endocrinol. 5, 941–950. 10.1016/S2213-8587(17)30313-3. [PubMed: 28927706]

Sahebkar A, Simental-Mendía LE, Guerrero-Romero F, Golledge J, and Watts GF (2015). Effect of statin therapy on plasma proprotein convertase subtilisin kexin 9 (PCSK9) concentrations: a systematic review and meta-analysis of clinical trials. Diabetes Obes. Metab 17, 1042–1055. 10.1111/dom.12536. [PubMed: 26183252]

Salunkhe VA, Elvstam O, Eliasson L, and Wendt A (2016). Rosuvastatin treatment affects both basal and glucose-induced insulin secretion in INS-1 832/13 cells. PLoS One 11, e0151592. 10.1371/journal.pone.0151592. [PubMed: 26986474]

Sattar N, Preiss D, Murray HM, Welsh P, Buckley BM, de Craen AJM, Seshasai SRK, McMurray JJ, Freeman DJ, Jukema JW, et al. (2010). Statins and risk of incident diabetes: a collaborative meta-analysis of randomised statin trials. Lancet 375, 735–742. 10.1016/S0140-6736(09)61965-6. [PubMed: 20167359]

Sattar N, Toth PP, Blom DJ, Koren MJ, Soran H, Uhart M, Elliott M, Cyrille M, Somaratne R, and Preiss D (2017). Effect of the proprotein convertase subtilisin/kexin type 9 inhibitor evolocumab on glycemia, body weight, and new-onset diabetes mellitus. Am. J. Cardiol 120, 1521–1527. 10.1016/j.amjcard.2017.07.047. [PubMed: 28844508]

Sattar NA, Ginsberg H, Ray K, Chapman MJ, Arca M, Averna M, Betteridge DJ, Bhatnagar D, Bilianou E, Carmena R, et al. (2014). The use of statins in people at risk of developing diabetes mellitus: evidence and guidance for clinical practice. Atheroscler. Suppl. 15, 1–15. 10.1016/j.atherosclerosissup.2014.04.001.

Schachter M (2005). Chemical, pharmacokinetic and pharmacodynamic properties of statins: an update. Fundam. Clin. Pharmacol 19, 117–125. 10.1111/j.1472-8206.2004.00299.x. [PubMed: 15660968]

Schmidt AF, Swerdlow DI, Holmes MV, Patel RS, Fairhurst-Hunter Z, Lyall DM, Hartwig FP, Horta BL, Hyppönen E, Power C, et al. (2017). PCSK9 genetic variants and risk of type

2 diabetes: a mendelian randomisation study. Lancet Diabetes Endocrinol. 5, 97–105. 10.1016/S2213-8587(16)30396-5. [PubMed: 27908689]

Sharabi K, Lin H, Tavares CDJ, Dominy JE, Camporez JP, Perry RJ, Schilling R, Rines AK, Lee J, Hickey M, et al. (2017). Selective chemical inhibition of PGC-1alpha gluconeogenic activity ameliorates type 2 diabetes. Cell 169, 148–160.e15. 10.1016/j.cell.2017.03.001. [PubMed: 28340340]

Spolitu S, Okamoto H, Dai W, Zadroga JA, Wittchen ES, Gromada J, and Ozcan L (2019). Hepatic glucagon signaling regulates PCSK9 and low-density lipoprotein cholesterol. Circ. Res 124, 38–51. 10.1161/CIRCRESAHA.118.313648. [PubMed: 30582457]

Stern JH, Smith GI, Chen S, Unger RH, Klein S, and Scherer PE (2019). Obesity dysregulates fasting-induced changes in glucagon secretion. J. Endocrinol 243, 149–160. 10.1530/JOE-19-0201. [PubMed: 31454790]

Swerdlow DI, Preiss D, Kuchenbaecker KB, Holmes MV, Engmann JEL, Shah T, Sofat R, Stender S, Johnson PCD, Scott RA, et al. (2015). HMG-coenzyme A reductase inhibition, type 2 diabetes, and body-weight: evidence from genetic analysis and randomised trials. Lancet 385, 351–361. 10.1016/S0140-6736(14)61183-1. [PubMed: 25262344]

Takahashi H, Shibasaki T, Park JH, Hidaka S, Takahashi T, Ono A, Song DK, and Seino S (2015). Role of Epac2A/Rap1 signaling in interplay between incretin and sulfonylurea in insulin secretion. Diabetes 64, 1262–1272. 10.2337/db14-0576. [PubMed: 25315008]

Taylor BA, and Thompson PD (2016). Statins and their effect on PCSK9-impact and clinical relevance. Curr. Atheroscler. Rep 18, 46. 10.1007/s11883-016-0604-3. [PubMed: 27315084]

Unger RH, and Cherrington AD (2012). Glucagonocentric restructuring of diabetes: a pathophysiologic and therapeutic makeover. J. Clin. Invest 122, 4–12. 10.1172/JCI60016. [PubMed: 22214853]

Vella A, Freeman JLR, Dunn I, Keller K, Buse JB, and Valcarce C (2019). Targeting hepatic glucokinase to treat diabetes with TTP399, a hepatoselective glucokinase activator. Sci. Transl. Med 11, eaau3441. 10.1126/scitranslmed.aau3441. [PubMed: 30651321]

Wang H, Wang AX, and Barrett EJ (2012a). Insulin-induced endothelial cell cortical actin filament remodeling: a requirement for trans-endothelial insulin transport. Mol. Endocrinol 26, 1327–1338. 10.1210/me.2012-1003. [PubMed: 22734037]

Wang JC, Lee JYJ, Christian S, Dang-Lawson M, Pritchard C, Freeman SA, and Gold MR (2017). The Rap1-cofilin-1 pathway coordinates actin reorganization and MTOC polarization at the B cell immune synapse. J. Cell Sci 130, 1094–1109. 10.1242/jcs.191858. [PubMed: 28167682]

Wang L, Zhu L, Zheng Z, Meng L, Liu H, Wang K, Chen J, Li P, and Yang H (2022). Mevalonate pathway orchestrates insulin signaling via RAB14 geranylgeranylation-mediated phosphorylation of AKT to regulate hepatic glucose metabolism. Metabolism 128, 155120. 10.1016/j.metabol.2021.155120. [PubMed: 34995578]

Wang X, Cai B, Yang X, Sonubi OO, Zheng Z, Ramakrishnan R, Shi H, Valenti L, Pajvani UB, Sandhu J, et al. (2020). Cholesterol stabilizes TAZ in hepatocytes to promote experimental non-alcoholic steatohepatitis. Cell Metab. 31, 969–986.e7. 10.1016/j.cmet.2020.03.010. [PubMed: 32259482]

Wang Y, Li G, Goode J, Paz JC, Ouyang K, Screaton R, Fischer WH, Chen J, Tabas I, and Montminy M (2012b). Inositol-1, 4, 5-trisphosphate receptor regulates hepatic gluconeogenesis in fasting and diabetes. Nature 485, 128–132. 10.1038/nature10988. [PubMed: 22495310]

Wittchen ES, Aghajanian A, and Burridge K (2011). Isoform-specific differences between Rap1A and Rap1B GTPases in the formation of endothelial cell junctions. Small GTPases 2, 65–76. 10.4161/sgtp.2.2.15735. [PubMed: 21776404]

Xu H, Ryan KA, Jaworek TJ, Southam L, Reid JG, Overton JD, Baras A, Puurunen MK, Zeggini E, Taylor SI, et al. (2017). Familial hypercholesterolemia and type 2 diabetes in the old order amish. Diabetes 66, 2054–2058. 10.2337/db17-0173. [PubMed: 28428224]

Highlights

- The hepatocyte small GTPase Rap1a suppresses gluconeogenesis via the Akt-FoxO1 pathway
- Restoring hepatic Rap1a activity improves obesity-associated glucose intolerance
- Rap1a is inhibited by the geranylgeranylation inhibitor statin in hepatocytes and liver
- Geranylgeraniol treatment improves statin-induced glucose intolerance

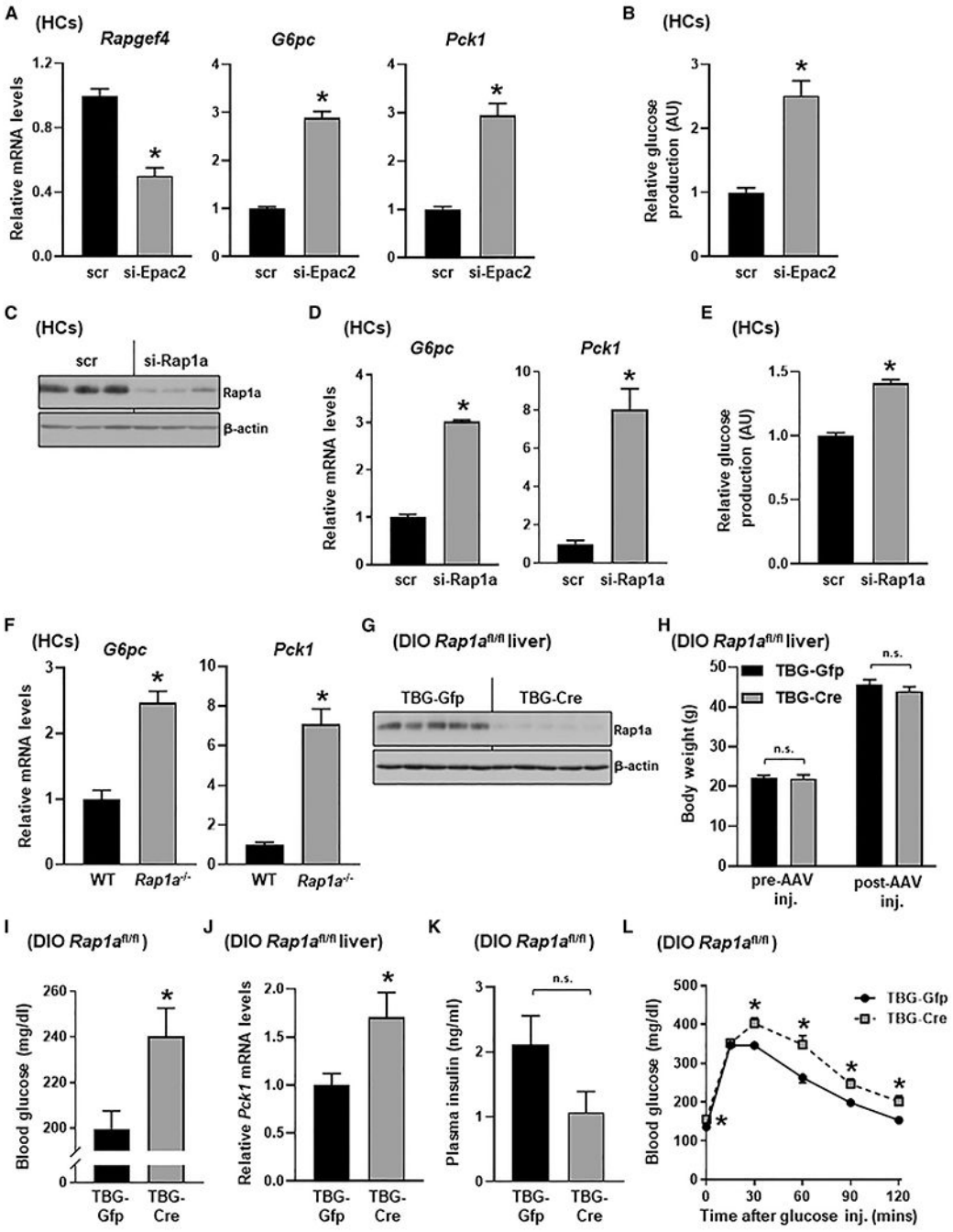

Figure 1. Inhibition of Epac2 or Rap1a stimulates gluconeogenesis and increases hepatocyte glucose production

(A) *Rapgef4* (Epac2), *G6pc*, and *Pck1* mRNA levels were analyzed from forskolin and dexamethasone (F + D)-treated primary mouse hepatocytes (HCs) that were transfected with scrambled RNA (scr) or siRNA against Epac2 (si-Epac2) (n = 4 biological replicates, mean ± SEM, *p < 0.05).

(B) Same as in (A), except that glucose production was measured (n = 4 biological replicates, mean ± SEM, *p < 0.05).

(C–E) Rap1a and β-actin levels (C), *G6pc* and *Pck1* mRNA (D), and glucose production (E) from F + D-treated primary mouse hepatocytes that were transfected with scrambled RNA (scr) or siRNA against Rap1a (si-Rap1a) (n = 3–4 biological replicates, mean ± SEM, *p < 0.05).

(F) *G6pc* and *Pck1* mRNA levels were measured from glucagon-treated WT or $Rap1a^{-/-}$ mouse hepatocytes (n = 6 biological replicates, mean ± SEM, *p < 0.05).

(G–L) Hepatic Rap1a and β-actin levels (G), body weight before and after AAV injection (H), 5-h fasting blood glucose (I), liver *Pck1* mRNA (J), 5-h fasting plasma insulin (K), and glucose tolerance test (L) from DIO $Rap1a^{fl/fl}$ mice that were injected with adeno-associated viruses containing either hepatocyte-specific TBG-Cre recombinase (TBG-Cre) or the control vector (TBG-Gfp) (n = 5–8 mice/group, mean ± SEM, *p < 0.05, n.s., non-significant). See also Figures S1 and S2.

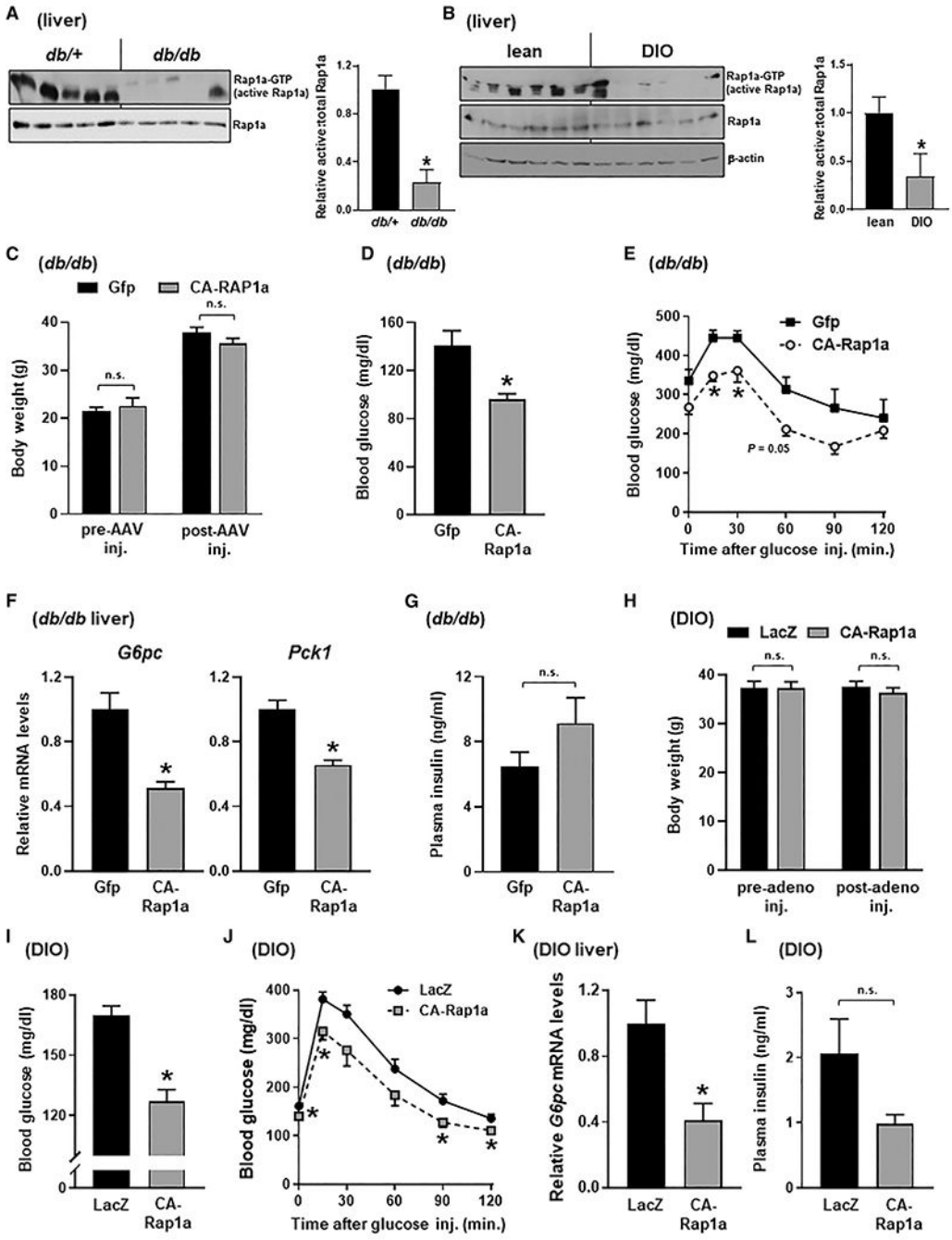

Figure 2. Activation of Rap1a is suppressed in obese mice liver, and restoring Rap1a activity lowers blood glucose and improves glucose intolerance in obese mice

(A) Livers from *db/db* and control (*db*/+) mice were assayed for GTP-bound (active) Rap1a and total Rap1a. Densitometric quantification of the immunoblot data is shown in the bar graph (n = 5 mice/group, mean ± SEM, *p < 0.05).

(B) Livers from DIO mice and their low-fat-fed controls (lean) were assayed for GTP-bound (active) Rap1a, total Rap1a, and β-actin. Densitometric quantification of the immunoblot data is shown in the bar graph (n = 6 mice/group, mean ± SEM, *p < 0.05).

(C–G) Body weight before and after AAV injection (C), overnight fasting blood glucose (D), glucose tolerance test (E), liver *G6pc* and *Pck1* mRNA (F), and overnight fasting plasma insulin (G) from *db/db* mice that were injected with adeno-associated viruses (AAV) containing either hepatocyte-specific CA-Rap1a (constitutively active Rap1a) or the control vector (Gfp) (n = 4–7 mice/group, mean ± SEM, *p < 0.05, n.s., non-significant).
(H–L) Body weight before and after adenovirus injection (H), 5-h fasting blood glucose (I), glucose tolerance test (J), liver *G6pc* mRNA (K), and 5-h fasting plasma insulin (L) levels from DIO mice that were injected with adenovirus vectors containing CA-Rap1a or control LacZ (β-galactosidase) (n = 6 mice/group, mean ± SEM, *p < 0.05, n.s., non-significant).

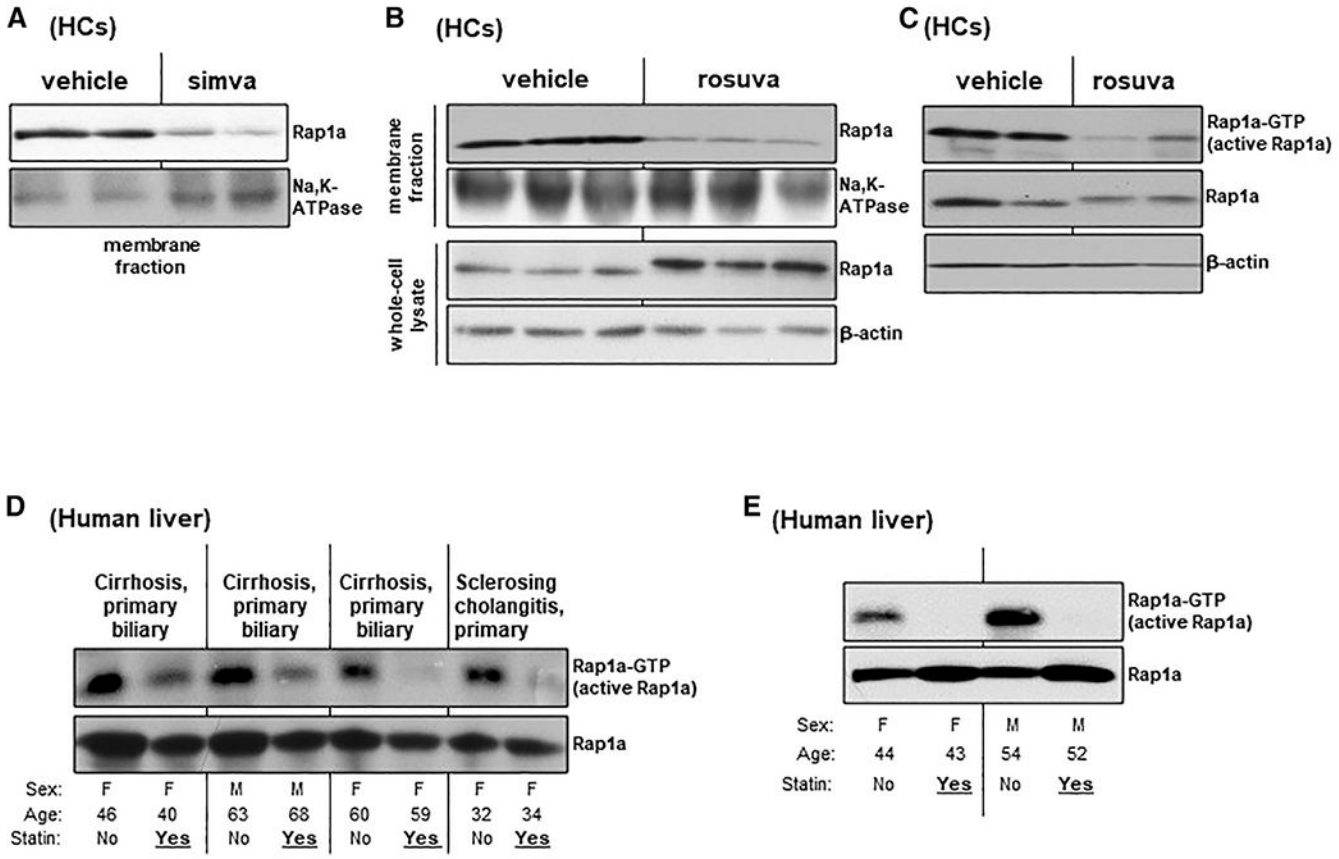

Figure 3. Statins inhibit Rap1a in isolated hepatocytes and the human liver

(A) Primary mouse hepatocytes (HCs) were treated with vehicle or 10 μM simvastatin (simva) for 20 h. Membrane proteins were assayed for Rap1a and Na, K-ATPase (loading control) (n = 2 biological replicates).

(B) Same as in (A), except that 5 μM rosuvastatin (rosuva) was used, and membrane fractions and whole-cell lysates were assayed for Rap1a and loading controls (Na, K-ATPase and μ-actin, respectively) (n = 3 biological replicates).

(C) Hepatocytes treated as in (B) were assayed for GTP-bound (active) Rap1a and total Rap1a (n = 2 biological replicates).

(D) Liver tissue samples from patients on statin therapy and their sex-, age-, and disease-matched controls without statin therapy were assayed for GTP-bound (active) Rap1a and total Rap1a (n = 4 human liver samples/group).

(E) Same as in (D), except that livers from another set of patients were assayed for GTP-bound (active) Rap1a and total Rap1a (n = 2 human liver samples/group).

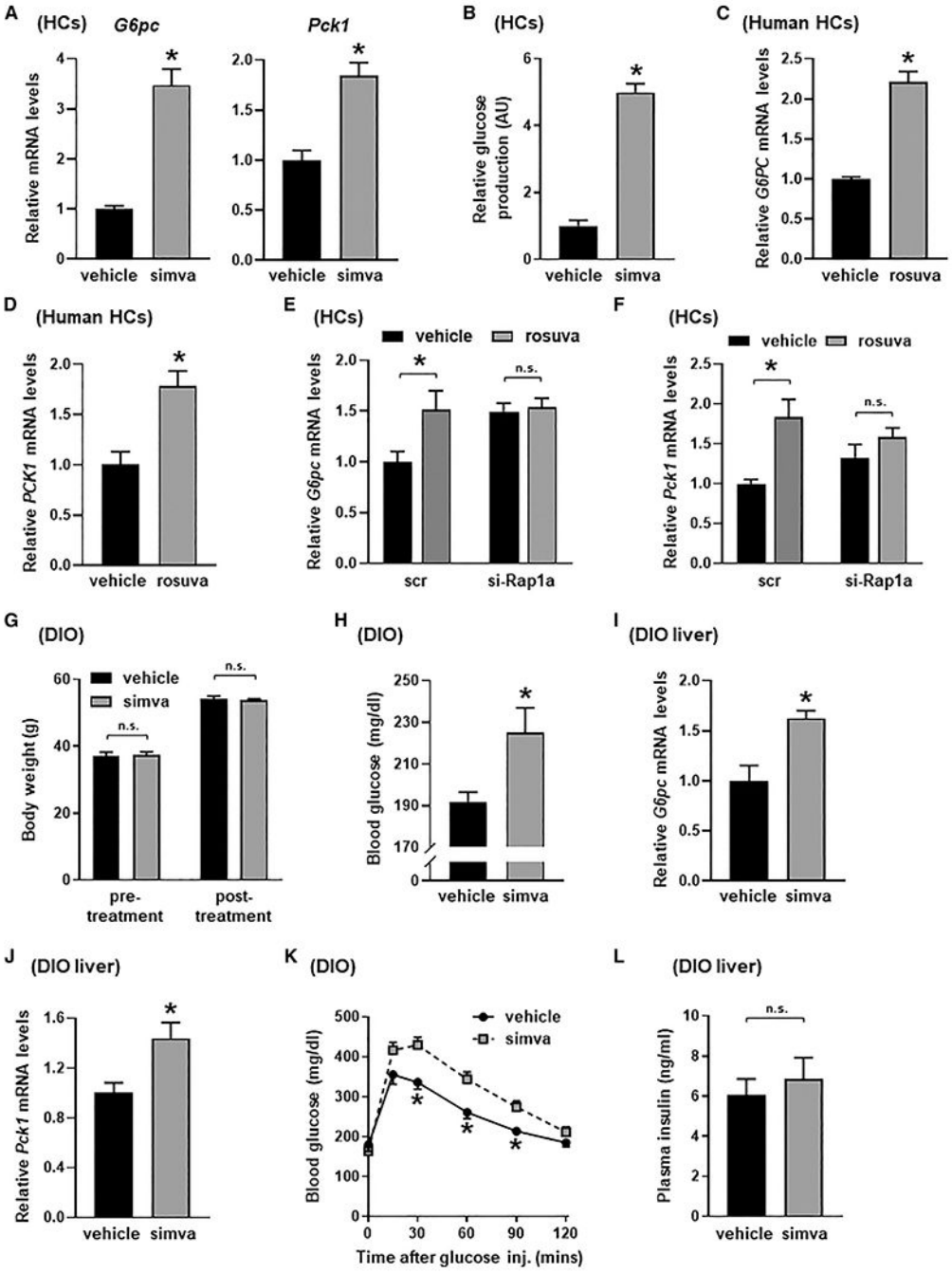

Figure 4. Statins increase gluconeogenesis in WT but not in *Rap1a*$^{-/-}$ hepatocytes

(A and B) Primary mouse hepatocytes (HCs) were treated with vehicle or 10 μM simvastatin (simva) for 24 h. The cells were then assayed for forskolin and dexamethasone (F + D)-induced *G6pc* and *Pck1* mRNA (A) and glucose production (B) (n = 4 biological replicates, mean ± SEM, *p < 0.05).

(C and D) F + D-induced *G6PC* (C) and *PCK1* (D) mRNAs were measured from human primary hepatocytes treated with vehicle control or 5 μM rosuvastatin (rosuva) for 24 h (n = 4 biological replicates, mean ± SEM, *p < 0.05).

(E and F) Primary mouse hepatocytes that were transfected with scrambled control (scr) or siRNA against Rap1a (si-Rap1a) were treated with vehicle or 5 μM rosuvastatin (rosuva) for 24 h. F + D-induced *G6pc* (E) and *Pck1* mRNA levels (F) were assayed (n = 3 biological replicates, mean ± SEM, *p < 0.05, n.s., non-significant).

(G–L) Body weight before and after the simvastatin treatment (G), 5-h fasting blood glucose (H), liver *G6pc* (I) and *Pck1* (J) mRNA, glucose tolerance test (K), and 5-h fasting plasma insulin (L) levels from DIO mice that were fed with a high-fat diet containing 0.02% simvastatin (w/w) (simva) for 12 weeks (n = 6–7 mice/group, mean ± SEM, *p < 0.05, n.s., non-significant). See also Figure S3.

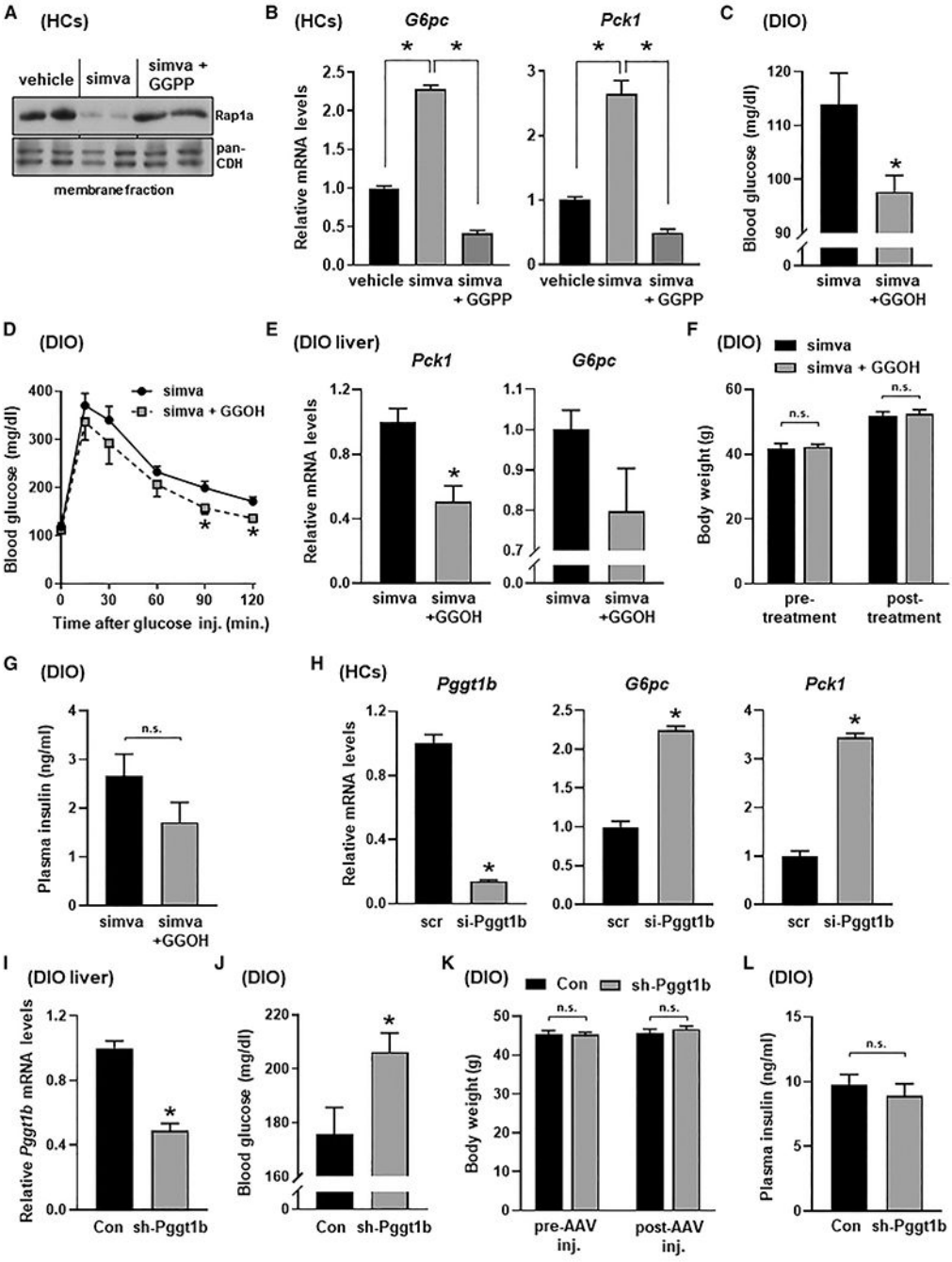

Figure 5. Geranylgeranylation mediates the gluconeogenic effect of statins

(A and B) Primary mouse hepatocytes (HCs) were treated with vehicle, 10 μM simvastatin (simva), or simvastatin + geranylgeranyl pyrophosphate (GGPP) (10 μM) for 24 h. Membrane proteins were assayed for Rap1a and pan-cadherin (pan-CDH, loading control) (A), and forskolin and dexamethasone (F + D)-induced *G6pc* and *Pck1* mRNA levels were measured (B) (n = 2–3 biological replicates, mean ± SEM, *p < 0.05).

(C–G) DIO mice were fed with a high-fat diet containing 0.02% simvastatin (w/w) for 12 weeks. Mice were then administered with geranylgeraniol (GGOH, 100 mg/kg/day) or

vehicle control by daily gavage for 3 weeks while still receiving the statin-containing diet. Overnight fasting blood glucose (C), glucose tolerance test (D), liver *G6pc* and *Pck1* mRNA (E), body weight before and after simvastatin and GGOH treatment (F), and overnight fasting plasma insulin (G) were assayed (n = 5–7 mice/group, mean ± SEM, *p < 0.05, n.s., non-significant).

(H) Primary mouse hepatocytes that were transfected with si-Pggt1b (encoding GGT1) or scrambled control (scr) were assayed for *Pggt1b*, and F + D-induced *G6pc and Pck1* mRNA levels (n = 3 biological replicates, mean ± SEM, *p < 0.05).

(I–L) Liver *Pggt1b* mRNA (I), 5-h fasting blood glucose (J), body weight before and after AAV injection (K), and 5-h fasting plasma insulin (L) levels were assayed from DIO mice that were injected with AAV8 vectors containing shRNA against Pggt1b (sh-Pggt1b) or empty, control AAV8 (Con) (n = 7 mice/group, mean ± SEM, *p < 0.05, n.s., non-significant). See also Figures S4–S6.

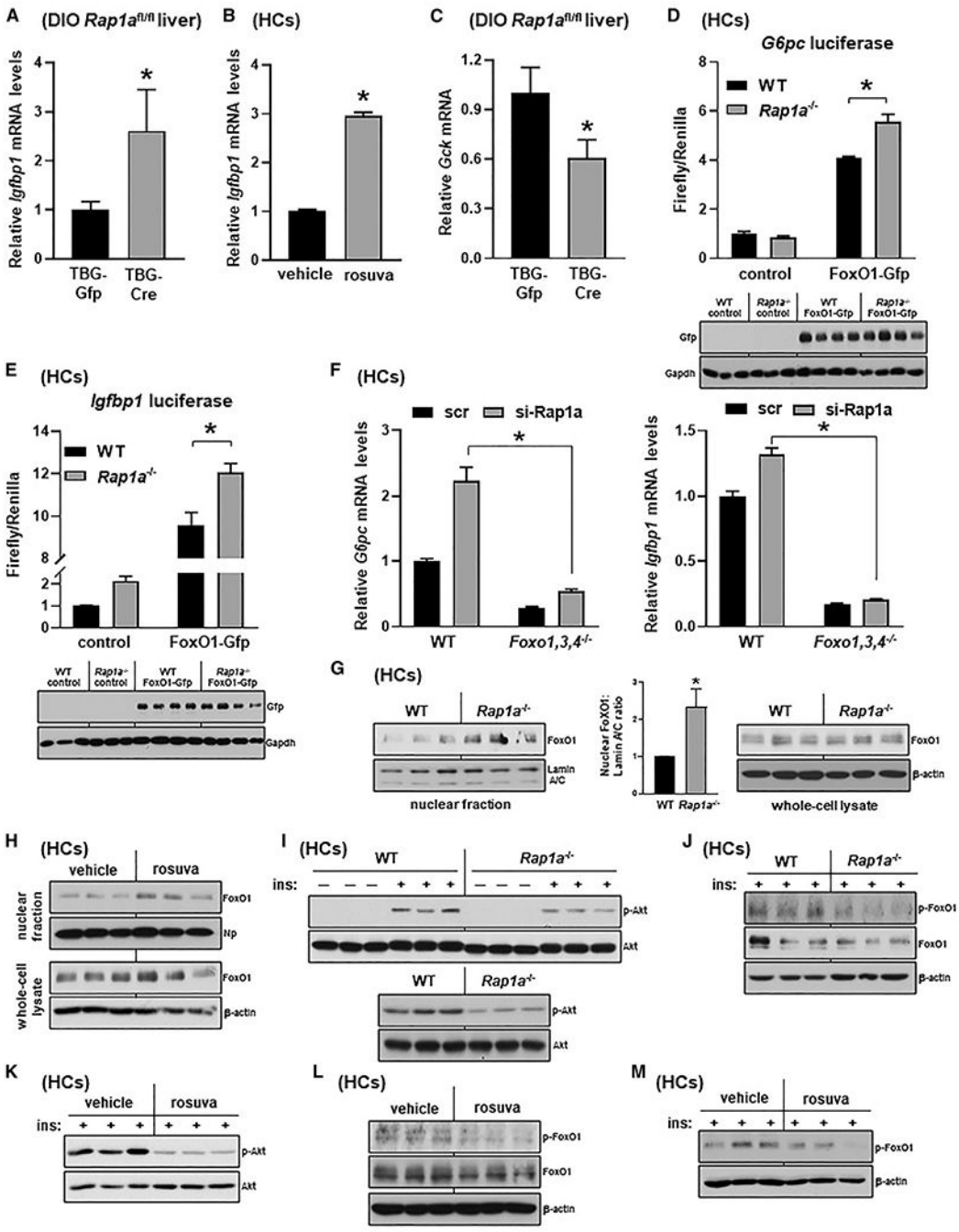

Figure 6. Rap1a inhibition or statin treatment increases gluconeogenesis via regulating FoxO1 activity

(A and B) *Igfbp1* mRNA levels were measured from the livers of DIO *Rap1a*$^{fl/fl}$ mice that were injected with TBG-Cre or TBG-Gfp (A), and vehicle- or 5 μM rosuvastatin (rosuva)-treated primary hepatocytes (HCs) that were incubated with forskolin and dexamethasone (F + D) (B) (n = 7–8 mice/group and n = 3 biological replicates, respectively, mean ± SEM, *p < 0.05).

(C) *Gck* mRNA levels were measured from the livers of DIO *Rap1a*$^{fl/fl}$ mice that were injected with TBG-Cre or TBG-Gfp (n = 7–8 mice/group, mean ± SEM, *p < 0.05).

(D) WT and *Rap1a*$^{-/-}$ primary hepatocytes were transfected with a luciferase fusion construct encoding nucleotides −1,227 to +57 of the *G6pc* promoter containing an intact FoxO binding site and FoxO1-Gfp or control plasmid. Relative luciferase activity and Gfp levels from WT and *Rap1a*$^{-/-}$ cells transfected with FoxO1-Gfp were measured (lower blots) (n = 3–4 biological replicates, mean ± SEM, *p < 0.05).

(E) Luciferase reporter assay of the *Igfbp1* promoter in WT and *Rap1a*$^{-/-}$ cells transfected with control or FoxO1-Gfp. Gfp levels from WT and *Rap1a*$^{-/-}$ cells transfected with FoxO1-Gfp were assayed in the lower blots (n = 3–4 biological replicates, mean ± SEM, *p < 0.05).

(F) *G6pc* and *Igfbp1* mRNA levels from F + D-treated WT and *Foxo1,3,4*$^{-/-}$ cells that were transfected with scrambled RNA (scr) or siRNA against Rap1a (si-Rap1a) (n = 4 biological replicates, mean ± SEM, *p < 0.05).

(G) Nuclear and whole-cell FoxO1 levels along with loading controls (lamin A/C and β-actin, respectively) in WT versus *Rap1a*$^{-/-}$ hepatocytes. Densitometric quantification of the nuclear FoxO1 immunoblot data is shown in the bar graph (n = 3 biological replicates).

(H) Nuclear and whole-cell FoxO1 levels along with loading controls (nucleophosmin, Np, and β-actin, respectively) in vehicle or 5 μM rosuvastatin (rosuva)-treated cells (n = 3 biological replicates).

(I) WT and *Rap1a*$^{-/-}$ hepatocytes were stimulated with vehicle control or insulin (100 nM) for 5 min, and p-Akt and total Akt levels were assayed (upper blots). Basal levels of phospho-Akt and total Akt in WT and *Rap1a*$^{-/-}$ cells are shown in the lower blots (n = 3 biological replicates).

(J) Same as in (I) except that p-FoxO1, total FoxO1, and β-actin levels were measured (n = 3 biological replicates).

(K–M) Vehicle or 5 μM rosuvastatin-treated cells were incubated with or without insulin (100 nM) for 5 min as indicated. p-Akt and total Akt (K), and p-FoxO1, total FoxO1, and β-actin levels (L–M) were assayed (n = 3 biological replicates). See also Figure S7.

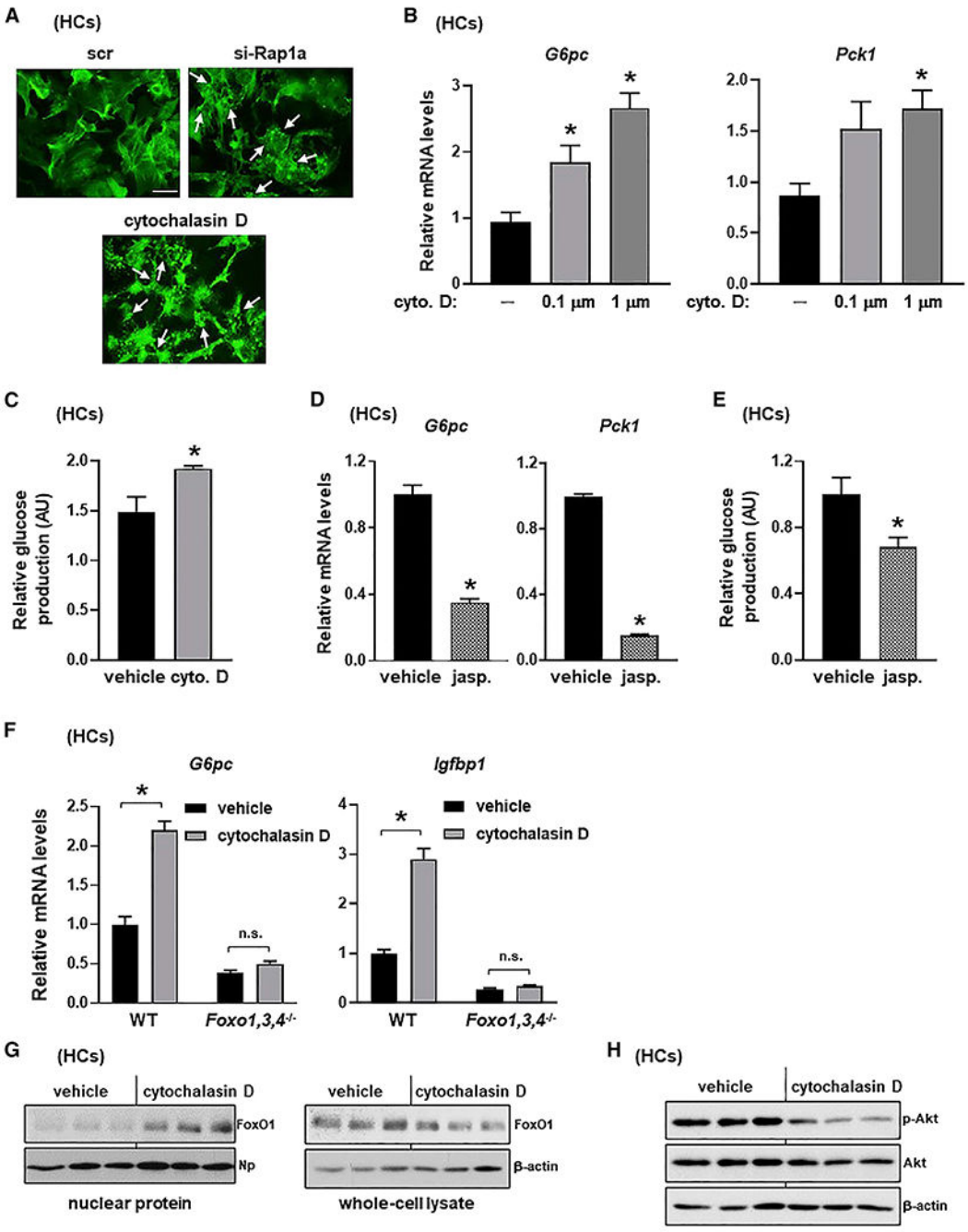

Figure 7. Actin remodeling contributes to gluconeogenesis and glucose production

(A) Primary mouse hepatocytes (HCs) that were treated with scrambled control (scr), si-Rap1a, or cytochalasin D were stained with 488-phalloidin (green) to visualize F-actin. White arrows indicate fragmented F-actin filaments that form cytoskeletal clumps. Scale bar, 10 μm.

(B) Hepatocytes were treated with vehicle, 0.1 μM, or 1 μM cytochalasin D (cyto. D) for 8 h, and forskolin and dexamethasone (F + D)-stimulated *G6pc* and *Pck1* mRNA levels were measured (n = 4 biological replicates, mean ± SEM, *p < 0.05).

(C) Same as in (B) except that glucose production was measured in cells treated with vehicle or 0.1 μM cytochalasin D (cyto. D) (n = 3 biological replicates, mean ± SEM, *p < 0.05).
(D) Hepatocytes were treated with 0.1 μM jasplakinolide (jasp.) for 6 h, and F + D-stimulated *G6pc* and *Pck1* mRNA levels were measured (n = 3 biological replicates, mean ± SEM, *p < 0.05).
(E) Same as in (D), except that glucose production was measured (n = 4 biological replicates, mean ± SEM, *p < 0.05).
(F) WT and *Foxo1,3,4*$^{-/-}$ hepatocytes were treated with vehicle or 1 μM cytochalasin D for 8 h, and F + D-stimulated *G6pc* and *Igfbp1* mRNA levels were measured (n = 4 biological replicates, mean ± SEM, *p < 0.05, n.s., non-significant).
(G) Nuclear and whole-cell FoxO1 levels along with loading controls (nucleophosmin, Np, and β-actin, respectively) were assayed in hepatocytes that were treated with vehicle or 1 μM cytochalasin D for 8 h (n = 3 biological replicates).
(H) Same as in (G), except that cells were stimulated with insulin, and p-Akt, total Akt, and β-actin levels were assayed (n = 3 biological replicates).

KEY RESOURCES TABLE

REAGENT or RESOURCE	SOURCE	IDENTIFIER
Antibodies		
Rabbit anti-β-actin	Cell Signaling Technology	Cat # 4970 RRID: AB_2223172
Rabbit anti-pan-Cadherin	Cell Signaling Technology	Cat # 4068 RRID: AB_2158565
Rabbit anti-GFP	Cell Signaling Technology	Cat # 2956 RRID: AB_1196615
Rabbit anti-GAPDH	Cell Signaling Technology	Cat # 5174 RRID: AB_10622025
Rabbit anti-p-Akt	Cell Signaling Technology	Cat # 4060 RRID: AB_2315049
Rabbit anti-Akt	Cell Signaling Technology	Cat # 4691 RRID: AB_915783
Rabbit anti-p-FoxO1	Cell Signaling Technology	Cat # 9464 RRID: AB_329842
Rabbit anti-FoxO1	Cell Signaling Technology	Cat # 2880 RRID: AB_2106495
Mouse anti-Lamin A/C	Cell Signaling Technology	Cat # 4777 RRID: AB_10545756
Rabbit anti-nucleophosmin (anti-NPM)	Cell Signaling Technology	Cat # 3542 RRID: AB_2155178
Rabbit anti-p-CREB	Cell Signaling Technology	Cat # 9198 RRID: AB_2561044
Rabbit anti-CREB	Cell Signaling Technology	Cat # 9197 RRID: AB_331277
Rabbit anti-p-PKA substrate	Cell Signaling Technology	Cat # 9624 RRID: AB_331817
Rabbit anti-HSP90	Cell Signaling Technology	Cat # 4877 RRID: AB_2233307
Goat anti-Rap1a	R&D Systems	Cat # AF3767 RRID: AB_622167
Rabbit anti-Na,K-ATPase	Abcam	Cat # ab76020 RRID: AB_1310695
Bacterial and virus strains		
AAV8-TBG-Gfp	Gene Therapy Resource Program (GTRP) of the NHLBI	N/A

REAGENT or RESOURCE	SOURCE	IDENTIFIER
AAV8-TBG-Cre	Gene Therapy Resource Program (GTRP) of the NHLBI	N/A
AAV8-TBG-Gfp	James M. Wilson	Addgene, Cat # 105535-AAV8
AAV8-TBG-Cre	James M. Wilson	Addgene, Cat # 107787-AAV8
AAV8-TBG-CA-Rap1a	Penn Vector Core	Custom
AAV8-H1-shPggt1b sense: (5'-CACCAAAGCCATCAGCTACATTAGAAGAAGTCAAGAGCTTCTTCTAATGTAGCTGATGGCTT-3')	Salk Institute Gene Transfer, Targeting, and Therapeutics Core	Custom
Adeno-LacZ	(Wittchen et al., 2011)	Custom
Adeno-CA-Rap1a	(Wittchen et al., 2011)	Custom
Biological samples		
Human liver samples	Liver Tissue Cell Distribution System at the University of Minnesota and Columbia University	N/A
Chemicals, peptides, and recombinant proteins		
Forskolin	Sigma-Aldrich	Cat # F6886
Dexamethasone	Sigma-Aldrich	Cat # D4902
Geranylgeranyl transferase 1 inhibitor (GGT1i)	Sigma-Aldrich	Cat # G5294
Geranylgeranyl transferase 1 inhibitor (GGT1i)	Sigma-Aldrich	Cat # G5169
Farnesyl transferase 1 inhibitor (FT1i)	Sigma-Aldrich	Cat # F9803
Glucose	Sigma-Aldrich	Cat # G7021
Glucagon	Sigma-Aldrich	Cat # G2044
Insulin	Sigma-Aldrich	Cat # I0516
Simvastatin	Sigma-Aldrich	Cat # S6196
Simvastatin	Tokyo Chemical Industry (TCI)	Cat # S0509

REAGENT or RESOURCE	SOURCE	IDENTIFIER
Rosuvastatin	Cayman Chemicals	Cat # 18813
Geranylgeranyl pyrophosphate (GGPP)	Cayman Chemicals	Cat # 63330
Geranylgeraniol (GGOH)	Cayman Chemicals	Cat # 13272
1,2-dimyristoyl-sn-glycero-3-phosphocholine (DMPC)	Avanti Polar Lipids	Cat # 850345
Cholesterol	Sigma-Aldrich	Cat # C8667
Heat-inactivated fetal bovine serum	GIBCO	Cat # 16140-071
DMEM/F12 medium	ThermoFisher Scientific	Cat # 11320033
Penicillin/streptomycin	Corning	Cat # 30-002-CI
Opti-MEM	ThermoFisher Scientific	Cat # 31985070
Lipofectamine RNAiMAX	ThermoFisher Scientific	Cat # 13-778-150
Lipofectamine 3000	ThermoFisher Scientific	Cat # L3000015
RIPA Buffer	ThermoFisher Scientific	Cat # PI89901
Supersignal West Pico enhanced chemiluminescent solution	ThermoFisher Scientific	Cat # PI34580
TRI Reagent	Sigma-Aldrich	Cat # T9424
Cryopreserved hepatocyte recovery medium	ThermoFisher Scientific	Cat # CM7000
Williams' Medium E	ThermoFisher Scientific	Cat # A1217601
Hepatocyte maintenance supplement pack	ThermoFisher Scientific	Cat # CM4000
Critical commercial assays		
Glucose (GO) Assay Kit	Sigma-Aldrich	Cat # GAGO20
Active Rap1 Detection Kit	Cell Signaling Technology	Cat # 8818
Cyclic AMP XP Assay Kit	Cell Signaling Technology	Cat # 4339
Phalloidin-iFluor 488 reagent	Abcam	Cat # ab176753
Ultrasensitive mouse insulin ELISA Kit	Crystal Chem	Cat # 90080
Dual-Luciferase Reporter Assay System	Promega	Cat # E1960
Nuclear Extract Kit	Active Motif	Cat # 40010
Experimental models: Cell lines		
Mouse: Primary hepatocytes	This paper	N/A
Human plateable hepatocytes	ThermoFisher Scientific	Cat # HMCPMS

REAGENT or RESOURCE	SOURCE	IDENTIFIER
AML12 cells	ATCC	Cat # CRL-2254
Experimental models: Organisms/strains		
Mouse: WT C57BL/6J	The Jackson Laboratory	JAX: 000664
Mouse: *db/db*	The Jackson Laboratory	JAX: 000697
Mouse: Diet-induced obese (DIO)	The Jackson Laboratory	JAX: 380050
Mouse: Controls for diet-induced obese	The Jackson Laboratory	JAX: 380056
Mouse: *Rap1a*$^{fl/fl}$ C57BL/6J	The Jackson Laboratory	JAX: 021066
Mouse: *Foxo1,3,4*$^{fl/fl}$	(Haeusler et al., 2010)	N/A
Oligonucleotides		
qPCR primers are listed in Table S1.	This paper	N/A
Mouse: IDT Rap1a DsiRNA sense: 5'-rCrArArGrCrUrArGrUrArGrUrCrCrUrUrGrGrUrUrCrArGGA-3'	Integrated DNA Technologies	Cat # mm.Ri.Rap1a.13.3
Mouse: IDT Rap1a DsiRNA antisense: 5'-rUrCrCrUrGrArArCrCrArArGrGrArCrUrArCrUrArGrCrUrUrGrUrA-3'	Integrated DNA Technologies	Cat # mm.Ri.Rap1a.13.3
Mouse: IDT Rapgef4 DsiRNA sense: 5'-rArArGrCrArArCrArGrArUrUrCrGrGrUrUrUrUrArArArUGA-3'	Integrated DNA Technologies	Cat # mm.Ri.RapGef4.13.3
Mouse: IDT Rapgef4 DsiRNA antisense: 5'-rUrCrArUrUrUrArArArArCrCrGrArArUrCrUrGrUrUrGrCrUrUrCrA-3'	Integrated DNA Technologies	Cat # mm.Ri.RapGef4.13.3
Mouse: IDT Pggt1b DsiRNA sense: 5'-rCrUrUrArArGrGrUrGrUrGrCrCrArArCrUrArArArCrArUGT-3'	Integrated DNA Technologies	Cat # mm.Ri.Pggt1b.13.2
Mouse: IDT Pggt1b DsiRNA antisense: 5'-rArCrArUrGrUrUrUrArGrUrUrGrGrCrArCrArCrCrUrUrArArGrArA-3'	Integrated DNA Technologies	Cat # mm.Ri.Pggt1b.13.2
Negative Control DsiRNA sense: 5'-rCrGrUrUrArArUrCrGrCrGrUrArUrArArUrArCrGrCrGrUAT	Integrated DNA Technologies	Cat # 51-01-14-04
Negative Control DsiRNA antisense: 5'-rArUrArCrGrCrGrUrArUrUrArUrArCrGrCrGrArUrUrArArCrGrArC	Integrated DNA Technologies	Cat # 51-01-14-04
Recombinant DNA		
Igfbp1-promoter/pGL3	(Nakae et al., 2000)	Addgene, Cat # 12146
GFP-FoxO1	(Frescas et al., 2005)	Addgene, Cat # 17551
Renilla luciferase	(Chen and Prywes, 1999)	Addgene, Cat # 27163
Rap1-E63 (CA-Rap1a)	(Lafuente et al., 2004)	Addgene, Cat # 32698
Software and algorithms		

REAGENT or RESOURCE	SOURCE	IDENTIFIER
ImageJ	NIH	https://imagej.nih.gov/ij/
PRISM	GraphPad Software	Version 9
SigmaPlot	SigmaPlot	Version 14.0
Other		
High-fat high-calorie diet	Research Diets	Cat # D12492